Unterschrift des Betreuers

TU WIEN
TECHNISCHE
UNIVERSITÄT
WIEN
Vienna University of Technology

DIPLOMARBEIT

Normal equation combination of VLBI and SLR for CONT14

Ausgeführt am

Department für Geodäsie und Geoinformation

Forschungsgruppe Höhere Geodäsie

der Technischen Universität Wien

unter der Anleitung von

Univ. Prof. Dipl.-Ing. Dr.techn. Johannes Böhm

Projektass. Dipl.-Ing. Dr.techn. Hana Krasna

Projektass. Dipl.-Ing. BSc Bakk.techn. Jakob Franz Gruber

durch

Elias Niel, BSc

Matr. Nr.: 0927727

Landstraßer Hauptstraße 146

1030 Wien

Wien, April 2018

Unterschrift (Student)

Abstract

In this master thesis VLBI and SLR (SINEX-) data from a 15-day measurement campaign in 2014 are combined on the level of normal equation (NEQ). This combination method plays an import role for the generation of Terrestrial Reference Frames and follows an approach by the Deutsches Geodätisches Forschungsinstut (DGFI), which is considered as an alternative to the state-of-the art method used at the Institut Géographique National (IGN) (ITRF derivation on solution-level). Thereby, residuals (dX) for VLBI and SLR ground stations are estimated by the Least Squares Adjustment (LSA) method and added to given a-priori coordinates. Thus an own terrestrial reference system is generated. Therefore definitions of the geodetic datum are tested. The two space geodetic techniques are connected via local ties at four Co-Location sites. They are implemented to the NEQs as conditions, fixing the distance between the respective observing units.

The results are investigated with respect to differences between VLBI and SLR stations, as well as differences between the (inter-technique) combined solution and the technique specific individual solutions. It is shown that the VLBI system is more stable than the SLR system. However this is also based on the fact that the available VLBI data is more homogenous. Hence, they are also used for the definition of the geodetic datum. On average the residuals have a size of 1.5 cm, varying between and within the two techniques. Furthermore, the variation of scale between the systems was investigated. Results show that the radius of the earth (of approximated 6371 km) is about 1 cm longer in the VLBI system than in the SLR system. This indicates a difference in scale of 1.7 ppb, which is comparable to the results found by Altamimi et al. [2016] with the combination of VLBI and SLR data on solution level . This can contribute to a better understanding of technique specific characteristics, which are necesarry in order to improve the accuracy of a global TRF. This thesis also points out relevant parameters and their influences on the combination of VLBI and SLR NEQs. Challenging aspects that need to be considered like discrepancies between individual reference systems are discussed.

Kurzfassung

Im Rahmen dieser Masterarbeit wurden VLBI und SLR (SINEX-) Daten einer 15-tägigen Messkampagne auf Normalgleichungsebene kombiniert. Dieses Kombinationsverfahren beruht auf dem Ansatz des Deutsches Geodätisches Forschungsinstuts (DGFIs) zur Bestimmung eines Terrestrischen Bezugsrahmen und stellt eine Alternative zum gängigen Ansatz der Kombination auf Lösungsebene (Institut Géographique National (IGN), Bestimmung des ITRF auf Lösungsebene) dar. Dabei werden Residuen (dX) für VLBI und SLR Bodenstationen mit der Methode der kleinsten Quadrate (LSA) geschätzt und an den gegebenen a-priori Koordinaten angebracht. Demzufolge wird ein eigenes Bezugssystem geschaffen, bei dem unterschiedliche Definitionen des geodätischen Datums getestet werden. Die Systeme der beiden geodätischen Weltraumverfahren werden über terrestrisch bestimmte Differenzvektoren bei 4 Ko-Lokations Stationen verbunden. Diese gehen in die Normalgleichungen als Bedingung ein, und fixieren die Distanz zwischen den jeweiligen Messeinheiten. Die Ergebnisse werden in Bezug auf Unterschiede zwischen den VLBI- und SLR-Verfahren (verfahrensinterne Lösung), als auch zu der kombinierten Lösungen untersucht.

Es wird gezeigt, dass das VLBI-System als stabiler als das SLR-System zu werten ist. Das ist darauf zurückzuführen, dass die verfügbaren VLBI-Daten homogener sind. Deshalb werden diese auch zur Definition des geodätischen Datums der kombinierten Lösung herangezogen. Die dabei geschätzten Residuen betragen im Schnitt $1,5\ cm$. Dabei gibt es sowohl innerhalb der einzelnen Verfahren, als auch zwischen den beiden Verfahren Unterschiede. Des weiteren wurden Unterschiede der Maßstäbe in den verschiedenen Systemen untersucht. Dabei zeigte sich, dass der Erdradius (genähert $6371\ km$) im VLBI-System um rund $1\ cm$ länger ist als im SLR-System. Das bedeutet einen relativen Maßstabsunterschied zwischen den beiden Systemen von $1.7\ ppb$. Unterschiede in dieser Größenordnung wurden ebenso bei der VLBI und SLR Kombination auf Lösungsebene festgestellt [Altamimi et al., 2016]. Diese Erkenntnis kann zum besseren Verständnis der verfahrenseigenen Spezifikationen beitragen, welche wiederum notwendig für die Verbesserung der Genauigkeit von globalen terrestrischen Bezugssystemen sind. Weiters werden im Zuge dieser Arbeit Parameter ausgemacht, die als Stellschrauben bei der Kombination von VLBI und SLR Normalgleichungen wirken. Ebenso wird auf dabei

zu berücksichtigende Herausforderungen, wie beispielsweise die Unterschiede zwischen einzelnen Bezugssystemen hingewiesen.

Acknowledgement

The time as a student and especially while working on this thesis taught me a lot in various aspects. In particular I learned to appreciate the scientific approach to challenges and the constant analysis and evaluation, which I want to pursue in my future life.

I want to thank my supervisor Johannes Böhm for the patient and always adjuvant and well-directed assistance throughout the whole working process! Likewise I appreciated the valuable support from Jakob Gruber and Hana Krasna, thank you!

Further I want to thank my colleagues and friends for the accompany and a great study period!

Above all, my biggest thank goes to my parents for their patient and great support throughout the course of all my studies!

Contents

Contents

1. Introduction and motivation

The earth rotates, the earth moves and the earth changes its shape. Some of the driving forces are due to interactions with external bodies like the sun or the moon. Other forces are due to earthquakes, motions of the earth's liquid core, volcanic eruptions, melting and freezing of large amounts of water and other earth-based sources.

On the other hand, we assume that maps define positions of certain locations precisely by coordinates, and that navigation systems stay reliable over time. How does the constantly moving earth relate to such a coordinate system? The topographic changes of locations on earth are relatively small, but still they have an effect in normal life. Also, the exact position of satellites in space relative to the earth's surface is of great importance for precise navigation systems like GPS and for remote sensing applications. The investigation and modeling of small but important changes are therefore an important field of research. The coordinate system for the earth ("geodetic reference system") has to be constantly adjusted. There are several methods to determine such a reference system. They all have in common that measurements and observations with different geodetic techniques are combined and build a common framework. Further measurements and applications (e.g. positioning systems) can refer to this framework.

In this thesis, data from two space geodetic measurement techniques are combined: Very Long Baseline Interferometry (VLBI, see chapter 3.1) and Satellite Laser Ranging (SLR, see chapter 3.2). The data are from a two week measurement campaign in 2014 (CONT14) by a network of VLBI and SLR stations with known a-priori coordinates. The combination is performed on the level of normal equations. This is an approach that was first executed at the Deutsches Geodätisches Forschungsinstut (DGFI) and is understood as a complementation to the state-of-the art method for the generation of a terrestrial reference system (combination of solutions; ITRF at IGN). Normal equations appear in Least Squares Adjustment (LSA) solving overdetermined systems of equations with the objective of minimizing the residual errors. Normal equations and LSA will be described in detail in chapter 4.

The adjustment of a reference frame with given a-priori coordinates due to new measurements is determined by the residuals dX. Comparing dX for different scenarios (separate solutions for SLR and VLBI as well as for combined systems; different options of handling local ties, using the scale parameter as an independent (fixed) or dependent variable) leads to insights into possible influences and estimates of the size of errors. Altamimi et al. [2016] have shown that there is a difference in the scale parameter of about 1.3 *ppb*

between SLR and VLBI data that are both used for the ITRF. So far this difference is without explanation. Therefore, in this thesis the same difference is studied, using the alternative approach of combining normal equations (instead of combining solutions).

The results may contribute to a better understanding of potential errors in geodetic reference systems and help improving their accuracy. This is important for the upgrading of many different applications like satellite communication or space-based measurements of sea level changes due to global warming.

2. Reference Frames

Geodetic reference frames are based on the regulations of a respective reference system that regulates their formation and specifications. They are used for scientific but also practical applications. Basically one can distinguish between two sorts of systems: There are celestial (space fixed, the earth moves/rotates within the frame) and terrestrial (earth fixed) reference systems (frame moves/rotates along with the earth).

The International Terrestrial Reference System (ITRS) is developed by the International Earth Rotation and Reference Sytems Service (IERS) and describes conditions for an international (global) terrestrial reference frame, such as the International Terrestrial Reference Frame (ITRF) or the Deutscher geodätischer terrestrischer Referenzrahmen (DTRF). Both are products of the combination of data derived from four different space geodetic techniques (VLBI, SLR, GNSS, DORIS - see chapter 3) and represent an earth fixed (co-rotating) right-handed cartesian coordinate frame with the origin in the earth's center of mass, the Z-Axis directed towards the pole and a scale close to the SI meter [Gérard and Luzum, 2010]. The respective standards and requirements, but also the scientific and technological possibilities increase every year. Moreover, and at least evenly important, the earth underlies regular and irregular movements. Thus the reference frames have to be updated constantly. The goal (by Global Geodetic Observing System (GGOS)) is to reach a global accuracy rate below 0.1 mm/year in order to be able to detect and evaluate a sea-level change on a global basis [Glaser et al., 2017].

The ITRF and the DTRF differ in the way they are generated. In particular, the combination level of the space geodetic techniques' data is different. Generally, every technique has its own reference frame, determined by station coordinates and further specific values (see table 1).

There are three data-levels that all techniques have in common and where a combination can be performed [Seitz, 2015]:

- Combination of observations
- Combination of normal equation (NEQ)
- Combination of solutions

The ITRF is generated at the Institut Géographique National (IGN) in Paris, France and based on combining solutions of the different space geodetic techniques. Whereas the DTRF is developed at the DGFI in Munich, Germany and is based on the combination of normal equations NEQ of the respective space geodetic techniques' measurement's data.

A complete reference frame based on combination of observations has not been realized so far. There have been promising achievments by the "IERS Working Group on Combination at the Observation Level" (ceased in 2016). Its intended strategy is meant to be pursued to in order comply with the requirements for a new reference frame (which is needed for e.g. global change monitoring) [Hobiger and Otsubo, 2014]. However through the E-GRASP/Eratosthenes mission a new approach is being investigated and about to be started [Biancale Richard, Arnaud Pollet, David Coulot, 2017]. Its main innovation is the combination of all four space geodetic techniques measuring units in space in one satellite. This shall improve and facilitate their combination (now mainly via local ties on the ground).

3. Space geodetic techniques

As stated in chapter 2, data from four space geodetic techniques (VLBI, SLR, GNSS, DORIS) are combined, in order to generate a global terrestrial reference frame. And each of these techniques has its own reference frame. Nevertheless those individual reference frames differ slightly within each other due to technique-specific properties and specifications (see tab. 1) [Plank, 2016]. This section sums up the principles of each technique, presents their benefits and disadvantages, and discusses how they complement each other.

	VLBI	SLR	GNSS	DORIS
Station Coordinates	x	x	x	x
EOP				
- Pole Coord.	x	x	x	x
- δ UT1	x			
- Nutation	x			
Datum				
- Origin		x	(x)	(x)
- Scale	x	x	(x)	(x)

Table 1: Space geodetic techniques and their capabilities of retrieving parameters. (x) indicates, that the respective information is not used for the ITRF realization. Source: [Plank, 2016]

3.1. Very Long Baseline Interferometry (VLBI)

Very Long Baseline Interferometry (VLBI) is a passive measuring technique, that was originally developed for astronomy, but later was found as an important tool in space geodesy. The value of interest is the difference of arrival times between different receivers (connected through baselines) of radiowaves emitted by quasars. Quasars ("quasi-stellar") are extragalactic radiosources whose positions can be taken as fixed reference points. Due to the large distance between the emitter and the receivers related to the size of the Quasar and the length of the baselines, the incoming wavefronts can be taken as planar. Hence the determined time delay between two observatories $\tau_g = \tau_2 - \tau_1$ (geometric delay) is related to the length of the baseline b as illustrated in equation 1 and figure 1 [Schuh and Behrend, 2012]:
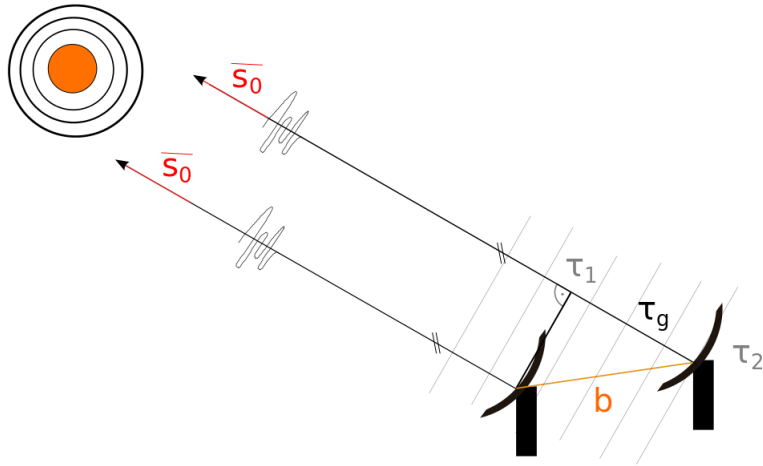
$$\tau_g = -\frac{b \cdot s_0}{c} \tag{1}$$

Figure 1: The basic principle of VLBI

c ... Speed of light
s_0 ... Unit vector between receiver and source
b ... Baseline vector

The time delay τ is resolved at correlation centers by the application of cross-correlation functions on time-tagged data, which are based on recorded signals within X-Band[1] and S-Band[2] [Schuh and Böhm, 2013]. The actual delay time is the geometric delay compounded with some additional delays caused by different physical effects shown in the observation equation (eq. 2):

$$\tau = \tau_g + \tau_{ab} + \tau_{clk} + \tau_{inst} + \tau_{trop} + \tau_{iono} + \tau_{rel} \tag{2}$$

---

[1]designated frequency spectrum for EM-Waves from 8-12 GHz, VLBI records at 8,4 GHz
[2]designated frequency spectrum for EM-Waves from 2-4 GHz, VLBI records at 2,3 GHz

τ_g ...   geometric delay
τ_{ab} ...   contribution due to diurnal abberation
τ_{clk} ...   contribution due to clock missynchronization
τ_{inst} ...   contribution due to delays in instrumentations
τ_{trop} ...   contribution due to delays through the troposphere
τ_{iono} ...   contribution due to delays through the ionosphere
τ_{rel} ...   contribution due to special and general relativistic corrections

VLBI provides the variation of the length of baselines over time. Further, as it refers to extragalactic sources (Quasars), it is the only space geodetic technique that can be used to determine all five Earth Orientation Parameters (EOP) and builds a complete connection between a celestial (space fixed) and a terrestrial (earth fixed) reference frame. [Takahashi, 2000]

3.2. Satellite Laser Ranging (SLR)

Satellite Laser Ranging (SLR) is an active two-way-ranging space geodetic technique that is capable of providing data for the determination of the gravity field, position coordinates and earth orientation parameters, as well es tidal information among others.

The value of interest is the two-way-travel time of laser pulses, which is direct proportional to the distance between the ground station and the satellite (see eq. 3 and fig. 2):

$$d_g = \frac{\delta t \cdot c}{2} \tag{3}$$

with

d_g ...   geometric distance between ground station and satellite
δt ...   two-way-travel time
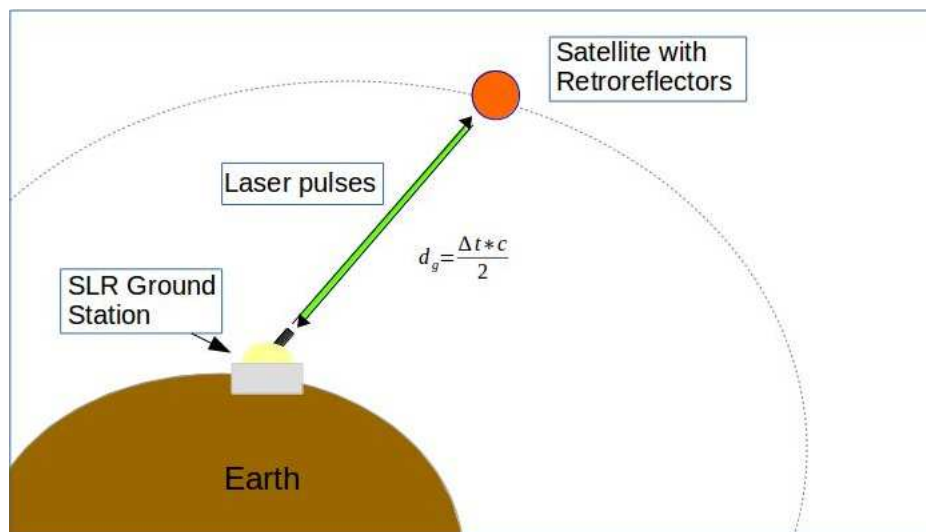c ...   speed of light

Figure 2: Measuring principle of SLR

However, to improve the accuracy of d_g further correction terms have to be added for the extended ranging equation [Seeber, 2003]:

$$d = d_g + \delta d_0 + \delta d_S + \delta d_b + \delta d_r + \eta \tag{4}$$

δd_0 ...   eccentricity correction on the ground
δd_S ...   eccentricitity correction at the satellite
δd_b ...   signal delay in the ground system
δd_r ...   refraction correction
η ...   remaining systematic and random observation errors

Laser pulses are emitted from the ground stations directly towards the satellites. They can be relatively light weighted and small as they only need retro-reflectors (see fig. 3), to reflect the signal back to earth, where it is recorded again. Due to the well known satellite orbits, station positions and their variations can be determined very precisely.
A big advantage, in addition to the little weight satellites, is that most of the technical infrastructure is at the ground stations, which makes the maintainance easy and does not depend on the complexity of satellites. A large number of satellites from other missions are also equiped with reflectors and can be aimed at by SLR emitters.

A disadvantage though, is that the measuring process and its accuracy depend considerably on current weather conditions. As the lasers use visible light, they are not able to penetrate clouds. Hence this technique works only with clear sky and ground stations

should only be built at locations with stable weather conditions. The station accuracy of SLR measurements goes hand in hand with the accuracy of the timer (clock), which needs to be at 1-2 ps for 1 mm for the location [Seeber, 2003]. As stated in table 1 SLR is practically the only method to measure the earth center of mass and in order to determine the origin of a TRF. Besides, SLR plays a major role in the determination of the earth gravity field (e.g. GRACE-Mission) [Thaller, 2008].

3.3. Global Navigation Satellite System (GNSS)

Global Navigation Satellite System (GNSS) is a general term for positioning services including GPS (USA), GLONASS (Russia), Galileo (Europe), or BeiDou/Compass (China). They are all based on the same principles, however work slightly different with respect to signal-frequencies, satellite constellations and regional accuracies. Besides Galileo, which is explicitly developed for civil services by the ESA in collaboration with the European Union and several other countries, all techniques have an originally major military purpose. The most comon and used service is defenitely the Global Positioning System (GPS), which will also be used to explain the basic principles in this chapter.

Figure 3: LAGEOS 1 - SLR Satellite with a diameter of 60 cm and 426 reflectors. Source: NASA

The basic principle of GNSS is, that a signal (EM-Wave with modulated information) is emitted by a satellite - forming spherical waves - and can be recorded and used for positioning by any GNSS receiver (aside from encrypted codes). There are two measuring concepts for GPS; namely code- and phase-measurements for course and fine position determination. With code-measurements, so called *Pseudoranges* are determined by runtime-measurements of the signal between the satellite and the receiver. Measurements from at least four satellites have to be taken into account, in order to determine a position (coordinate triple) on earth. Three to get a geometric intersection point out of three spheres and a fourth to overcome the receiver-clock-error, which appears because the receiver's clock is not synchronized with the emitter's clock on board of the satellite. Additional and necessary information, such as satellite-position, and meteorological data (to mention a few) is included in the navigation message which is modulated to the signal and can be extracted by the receiver.

In case of the more precise concept of phase measurement, the receiver records the phase

angle (compare modulo 2π) of the incoming signal when it hits the sensor. Although the integer number of cycles, the signal has passed since being emitted is not known ("*cycle ambiguities*"), this method yields a better resolution, as it can achieve an accuaracy of about 1% of the wavelength. There are several approaches to solve the ambiguities, comparing different phase offsets, as well as different frequencies. For civilian use, there are basically three different frequencies reserved for GPS (L1[3], L2[4], L5[5]). The GPS observation equation, describing influences on the signal on its path from the satellite to the receiver is given by (eq. 5 for code measurements and eq. 6 for carrier phase measurements) [Xu and Xu, 2016].

$$R_r^s = \rho_r^s(t_r, t_e) - (\delta t_r - \delta t_s)c + \delta_{ion} + \delta_{tro} + \delta_{tide} + \delta_{mul} + \delta_{rel} + \epsilon \tag{5}$$

$$\lambda \Phi_r^s(t_r) = \rho_r^s(t_r, t_s) - c(\delta t_r - \delta t_s) + \lambda N_r^s - \delta_{ion} + \delta_{tro} + \delta_{tide} + \delta_{mul} + \delta_{rel} + \epsilon \tag{6}$$

with

ρ_r^s geometrical distance between satellite and receiver

c speed of light

$c \cdot \delta t_r$ receiver clock error

$c \cdot \delta t^s$ satellite clock error

δ_{tro} tropospheric path dely

δ_{ion} ionospheric path dely

δ_{mul} multipath effects

δ_{tide} earth' tidal effects

δ_{rel} relativistic effects

ϵ remaining errors

λ wavelength

Φ_r^s carrier phase, emitted by satellite, recorded by receiver

N_r^s phase ambiguity between satellite and receiver

For the ITRF generation, GNSS provides station coordinates and pole coordinates.

---

[3]Signalfrequency at 1575,42 MHz
[4]Signalfrequency at 1227,60 MHz
[5]Signalfrequency at 1176,45 MHz

3.4. Doppler Orbitography and Radiopositioning Integrated by Satellite (DORIS)

DORIS is a French positioning system, that was developed by its national space agency (CNES) in order to determine satellite orbits and station positions on earth. Other than with GNSS, the signal (electromagnetic waves at a frequency of 2036.25 MHz and 401.25 MHz) is emitted by ground stations and received by satellites (uplink), which then send the recorded information-data back to earth.

The measuring principle of DORIS is based on the Doppler-Effect. When the receiver and the emitter move relatively to each other the recorded frequency is different than the emitted signal-frequency. If they move towards each other the received frequency is higher, if they move away from each other it is lower. If both frequencies are equal the satellites' track is exactly perpendicular above the ground station. Analyzing the course over time of the received frequencies from one satellite yields the distance between the receiver and the emitter.

Ground stations contain an omnidirectional beacon, a stable frequency oszillator, sensors for air pressure, air moisture and temperature, and have to be free of any shadowing effects. The emitted signal contains a modulated message including station ID, time and meteorolgical data.

DORIS as such provides a relatively young (developed in the 1980s) and small space geodetic service and works mainly as an addition to the established techniques (mentioned in section 3), but plays an important role in verifying and improving other solutions and products (for example the ITRF). A big advantage of DORIS is the homogenous station distribution around the globe, as well as the relatively simple and cheap installation and maintenance (receivers can be easily installed at satellites from other missions) [Böhm, 2014].

4. Mathematical background

The majority of the performed calculations is based on the principle of adjustment computation and specifically on the theory of Least Squares Adjustment (LSA). As stated in chapter 1 the individual datasets are combined on normal equation (NEQ) level (same as for the DTRF). Original data, in-between results and final results were evaluated through statistical values and transformation parameters. This chapter presents the mathematical methods and formulas for the data processing, which will be decscribed in chapter 6.

4.1. Least Squares Adjustment

Least Squares Adjustment (LSA) is a method to estimate parameters from redundant observations under the assumption that they are independent, normally distributed and free of outliers (thus it is a non robust method). It yields the minimization of square sum of the residual errors v_i (see eq. 4.1). The solution algorithm is based on the Gauss-Markoff Model (GM).

To start off, a functional model φ has to be set up to describe the theoretical link between the observations $\tilde{L}$ and the unknown parameters $\tilde{X}$ ($\sim$ denoting theoretical true values).

$$\tilde{L} = \varphi(\tilde{X}) \tag{7}$$

However, as in practice, the true values $\tilde{L}$ and $\tilde{X}$ are not known, they are represented by estimates $\hat{L}$ and $\hat{X}$. The adjusted observation estimates $\hat{L}$ are composed by the actual measurement observations L and the adjustments v ($\hat{L} = L + v$).

As the Gauss-Markoff Model requires the function φ to be linear, it is ususally approximated by the first-order terms of a Taylor-series expansion with apriori-values X_0. This linearized model is represented through the *Design-Matrix* A (see eq. 8). The value to be determined is Δx, representing the residuals to be applied upon X_0 ($\hat{X} = X_0 + \Delta x$). As the value of Δx is comparably small with respect to X_0, the values representing the observations have to be of the same size, which in order are represented through the shortened observation vector l ($L - L_0 = l$ with $L_0 = f(X_0)$, or "*observed - computed*").

$$A = \begin{bmatrix} \frac{\Delta\varphi_1}{\Delta X_1} & \frac{\Delta\varphi_1}{\Delta X_2} & \cdots & \frac{\Delta\varphi_1}{\Delta X_u} \\ \frac{\Delta\varphi_2}{\Delta X_1} & \frac{\Delta\varphi_2}{\Delta X_2} & \cdots & \frac{\Delta\varphi_2}{\Delta X_u} \\ \vdots & \vdots & \ddots & \vdots \\ \frac{\Delta\varphi_n}{\Delta X_1} & \frac{\Delta\varphi_n}{\Delta X_2} & \cdots & \frac{\Delta\varphi_n}{\Delta X_u} \end{bmatrix} \tag{8}$$

Hence, the basic equation to derive the residual errors v_i reads as follows

$$v = A \cdot \Delta x - l \qquad (9)$$

This equation can be solved by the LSA algorihtm demanding the minimization of the squared sum of the residual errors v_i:

$$v^T \cdot P \cdot v \Rightarrow min \qquad (10)$$

with the weight matrix P (inverse co-factor matrix Q_{ll} and variance factor σ_0^2),

$$Q_{ll} = \frac{1}{\sigma_0^2} \cdot \Sigma_{ll} \qquad (11)$$

$$P = Q_{ll}^{-1} \qquad (12)$$

and the co-variances σ_{ij} and the variances σ_i^2 forming the Co-variance matrix Σ_{ll}.

$$\Sigma_{ll} = \begin{bmatrix} \sigma_1^2 & \sigma_{12} & \sigma_{13} & \cdots & \sigma_{1i} \\ \sigma_{21} & \sigma_2^2 & \sigma_{23} & \cdots & \sigma_{2i} \\ \vdots & \vdots & \vdots & \ddots & \vdots \\ \sigma_{i1} & \sigma_{i2} & \sigma_{i3} & \cdots & \sigma_i^2 \end{bmatrix} \qquad (13)$$

Further, the application of the following formulas yields

$$N = A^T \cdot P \cdot A \qquad (14)$$

and

$$n = A^T \cdot P \cdot l \qquad (15)$$

for the derivation of estimates for Δx. This is accomplished by multiplying the inverse normal equation matrix N and right hand side vector n (see eq. 16). Note that N and n are of main interest for this thesis. N is a quadratic matrix with the dimension of the number of unknowns; n is a vector with the length of the number of unknowns.

$$\Delta x = N^{-1} \cdot n \qquad (16)$$

Further the apriori values X_0 can be adjusted by

$$\hat{X} = X_0 + \Delta x \tag{17}$$

To determine the residual errors v, Δx (from eq. 16) has to be inserted into equation 9. [Niemeier, 2008] and [Wolf and Ghilani, 1997]

4.2. Parameter reduction

In some cases it is useful to eliminate certain unknown parameters (e.g. non coordinate parameters) of a NEQ-System. In this thesis this was neccesarry to prepare the normal equations for the stacking process (see chapter 6). The reduction is accomplished through the application of the following formulas.

At first all elements of the NEQ-System have to be re-sorted into a pattern, where the parameters to be kept (x_1) and those to be eliminated (x_2) can be separated. Thus it can be written in a block structure and looks like equation 18

$$\begin{bmatrix} N_{11} & N_{12} \\ N_{21} & N_{22} \end{bmatrix}^{-1} \begin{bmatrix} n_1 \\ n_2 \end{bmatrix} = \begin{bmatrix} x_1 \\ x_2 \end{bmatrix} \tag{18}$$

or re-arranged and split

$$I : n_1 = N_{11} \cdot x_1 + N_{12} \cdot x_2$$

$$II : n_2 = N_{21} \cdot x_1 + N_{22} \cdot x_2.$$

Assuming that N_{22} is invertible, the second equation of eq. 18 can be converted to

$$x_2 = N_{22}^{-1} \cdot n_2 - N_{22}^{-1} \cdot N_{21} \cdot x_1. \tag{19}$$

In a next step inserting the derived x_2 into the first equation of eq. 18 yields

$$N_{11} \cdot x_1 + N_{12} \cdot x_2 = n_1 \tag{20}$$

$$N_{11} \cdot x_1 + N_{12} \cdot (N_{22}^{-1} \cdot n_2 - N_{22}^{-1} \cdot N_{21} \cdot x_2) = n_1$$

$$\underbrace{(N_{11} - N_{12} \cdot N_{22}^{-1} \cdot N_{21})}_{\overline{N_{11}}} \cdot x_1 = \underbrace{n_1 - N_{12} \cdot N_{22}^{-1} \cdot n_2}_{\overline{n_1}}$$

representing the reduced NEQ-Model marked through overlined variables

$$\overline{N_{11}} \cdot \overline{x_1} = \overline{n_1} \tag{21}$$

or

$$\overline{x_1} = \overline{N_{11}}^{-1} \cdot \overline{n_1} \tag{22}$$

containing only parameters of interest [Niemeier, 2008].

4.3. Reconstruction of free Normal Equations

Original Solution INdependent EXchange Format (SINEX) data can be constrained by the provider. This means that special conditions or modellings are added during the preprocessing and can lead to distortions and biases during further processing. In particular at the combination of datasets from different providers, or especially space geodetic techniques. If that is the case, decomposed normal equations still have to be derived. Therefore a-priori $(C(x,x))$ and a-posteriori $(C(\hat{x},\hat{x}))$ covariance matrices have to be available. Operating the following subtractions yields decomposed normal equations matrices which can be used for further applications:

$$N = \hat{\sigma}_0^2 \cdot C(\hat{x},\hat{x})^{-1} - \sigma_0^2 \cdot C(x,x)^{-1} \tag{23}$$

$$n = \hat{\sigma}_0^2 \cdot C(\hat{x},\hat{x})^{-1} \cdot \hat{x} \tag{24}$$

As the a-priori variance factor σ_0 is usually not given in the SINEX file, it can be set equal to the given $\hat{\sigma}_0^2$ [Angermann et al., 2004].

4.4. Combination methods

As stated in chapter 2 there are various approaches to combine data from different space geodetic techniques. For this thesis individual data (daily and technique wise) were combined on the level of NEQ.

Stacking normal equation matrices is achieved by summing up corresponding elements of the particular NEQ systems. Therefore the dimension of the stacked (combined) normal equation matrix has to equal the number of unique parameters appearing in all individ-

ual datasets. Rows and columns representing parameters, which do not appear in every normal equation have to be added and filled up with *zeros* in the respective matrices.

$$N_s = N_1 + N_2 + \cdots + N_n$$
$$n_s = n_1 + n_2 + \cdots + n_n$$

(25)

And by way of example with

$$N_1 = \begin{bmatrix} x^1_{11} & x^1_{12} & x^1_{13} & 0 \\ x^1_{21} & x^1_{22} & x^1_{23} & 0 \\ x^1_{31} & x^1_{32} & x^1_{33} & 0 \\ 0 & 0 & 0 & 0 \end{bmatrix} N_2 = \begin{bmatrix} x^2_{11} & 0 & x^2_{13} & x^2_{14} \\ 0 & 0 & 0 & 0 \\ x^2_{31} & 0 & x^2_{33} & x^2_{34} \\ x^2_{41} & 0 & x^2_{43} & x^2_{44} \end{bmatrix}$$

(26)

The stacked NEQ-System (eq. 25) can then be inverted to derive estimates for a combined solution (eq. 29).

However this approach is only valid under the assumption that all N_i have the same stochastic characteristics, which, in most cases, will not be guaranteed. Therefore the individual summands are weighted according to their respective variance factors σ_0^2 [Angermann et al., 2004].

$$\lambda_i = \frac{\sigma_0^2}{\sigma_{0i}^2}$$

(27)

Hence, the stacked normal equations N_s and right hand side vectors n_s are arranged as follows (eq. 28).

$$N_s = \lambda_1 \cdot N_1 + \lambda_2 \cdot N_2 + \cdots + \lambda_n \cdot N_n$$
$$n_s = \lambda_1 \cdot n_1 + \lambda_2 \cdot n_2 + \cdots + \lambda_n \cdot n_n$$

(28)

The stacked residuals Δx_s are then determined by equation 29.

$$\Delta x_s = N_s^{-1} \cdot n_s$$

(29)

4.5. Datum definition and constraining of parameters

A geodetic datum describes the location and characteristics for an assembly of adjusted coordinates in space. Therefore *origin, orientation* and *scale* have to be defined. It is

"a set of parameters and conventions that defines and realizes a coordinate system for geodetic control on a national or global scale. Nowadays realized by the 3-D Cartesian coordinates or 2-D geodetic coordinates of a network of control points" [Teunissen and Montenbruck, 2017]. Mathematically a point cloud, or the coordinate frame is fixed or constrained to particular conditions, which prevent normal equation matrices from being singular and therefore not invertible. To overcome this problem additional information $(Gx - c = 0)$ has to be added to the NEQ system. Nonetheless, every adjustment on the matrices yields changes within the agreement of the assembly of points. Hence there are different solution approaches (named *sufficient constraints, minimum constraints, non-distorting constraints, loose constraints*), varying in the way parts and relations of the system are distorted or preserved (inner geometry, particular coordinates, all points in the same way, or some more and some less).

Practically applied in this thesis and most common in geodesy, the datum definition is accomplished by extending the normal matrices N and right hand side vector n with following G-matrices (see eq. 32) applying no-net-translation (NNT) and no-net-rotation (NNR) conditions. It is basically a constraining method, minimizing the mean translation and rotation of the network with respect to a chosen set of a priori values [Angermann et al., 2004].

$$G = \begin{bmatrix} 1 & 0 & 0 & 0 & -z_0 & y_0 \\ 0 & 1 & 0 & z_0 & 0 & -x_0 \\ 0 & 0 & 1 & -y_0 & x_0 & 0 \end{bmatrix} \tag{30}$$

or

$$G = \begin{bmatrix} 1 & 0 & 0 & x_0 & 0 & -z_0 & y_0 \\ 0 & 1 & 0 & y_0 & z_0 & 0 & -x_0 \\ 0 & 0 & 1 & z_0 & -y_0 & x_0 & 0 \end{bmatrix} \tag{31}$$

to include the scale into the constraints.

$$N_c = \begin{bmatrix} N & G \\ G^T & 0 \end{bmatrix} \text{ and } n_c = \begin{bmatrix} n \\ 0 \end{bmatrix} \tag{32}$$

Relative constraints between parameters (local ties)

Similar to the definition of a geodetic datum, also relative constraints, which result from (pseudo-) observations L between certain parameters can be assigned. This can be a fixed angle between vectors or a fixed distance between points, such as the local ties fixing the distance between two observing units at a co-location site. These local ties are terrestrial measured vectors. Therefore a conditional equation $\varphi_c = f(L)$ has to be set up as a function of the observations representing the desired condition (constraint) mathematically. Analogous to the Design-Matrix A (see chapter 4.1) the partial derivations of φ_c with respect to observations, yields the conditional-Matrix B for m functions and n observations.

$$B = \begin{bmatrix} \frac{\partial \varphi_1}{\partial L_1} & \frac{\partial \varphi_1}{\partial L_2} & \cdots & \frac{\partial \varphi_1}{\partial L_n} \\ \frac{\partial \varphi_2}{\partial L_1} & \frac{\partial \varphi_2}{\partial L_2} & \cdots & \frac{\partial \varphi_2}{\partial L_n} \\ \vdots & \vdots & \ddots & \vdots \\ \frac{\partial \varphi_m}{\partial L_1} & \frac{\partial \varphi_m}{\partial L_2} & \cdots & \frac{\partial \varphi_m}{\partial L_n} \end{bmatrix} \tag{33}$$

The corresponding part on the right-hand side is a vector b, which represents the difference between the theoretical and the actual value of the denoted condition.

$$b = \varphi(L) \tag{34}$$

Thus according to Niemeier [2008] the functional model for the conditions (for the unknowns) is given by

$$B^T * \hat{x} = b \tag{35}$$

and can be added to the whole normal equation system as follows

$$\begin{bmatrix} N & B \\ B^T & 0 \end{bmatrix} \begin{bmatrix} \hat{x} \\ k \end{bmatrix} - \begin{bmatrix} n \\ b \end{bmatrix} = 0 \tag{36}$$

with the *Lagrange Multipliers k*.

4.6. Statistics

The final, as well as several intermediate results are evaluated by statistical analysis. Here is an overview of the concept used and their characteristics. The presented values always refer to a number of datapoints $L = (l_1, l_2, l_3, \ldots, l_i)$.

Mean

The most common value is the arithmetic mean. It is a non robust location estimator, which means that it is susceptible for outliers. Thus, outliers should be detected and eliminated beforehand. The actual value of the arithmetic mean $\bar{l}$ is usually not included in L and determined through

$$\bar{l} = \frac{1}{n} * (l_1 + l_2 + \cdots + l_n) = \frac{1}{n} * \sum_{i=1}^{n} l_i \tag{37}$$

Standard Deviation

The standard deviation σ (or std) is a measure for the dispersion of a set of data values. It describes how much the data speads out and it is defined as the square root of the variance σ^2.

$$\sigma = \sqrt{\sigma^2} = \sqrt{\frac{1}{n} * \sum_{i=1}^{n} (l_i - \bar{l})^2} \tag{38}$$

with the mean value $\bar{l}$.

Root Mean Square Error

The root mean square error $rmse$ is a value often used in technical engineering to compare datasets, representing the same parameters [Pontius et al., 2008]. It is defined as the square root of the average of squared errors.

$$rmse = \sqrt{\frac{1}{n} * \sum_{i=1}^{n} l^2} \tag{39}$$

with l being the difference of the parameters between two datasets.

$$l = x_1 - x_2 \tag{40}$$

Error Propagation

Often, the actual value of interest cannot be measured directly. Instead it is calculated as a function of variables, which come along with uncertainties due to measurement limitations. The resulting uncertainty of the final result can be determined by the *Gaussian*

error propagation law. The basic assumption therefore is, that the errors are normally distributed and free of outliers [Niemeier, 2008].

$$\sigma_f = \sqrt{\left(\frac{\partial_f}{\partial_{x_1}} * \sigma_{x_1}\right)^2 + \left(\frac{\partial_f}{\partial_{x_2}} * \sigma_{x_2}\right)^2 + \cdots + \left(\frac{\partial_f}{\partial_{x_n}} * \sigma_{x_n}\right)^2} = \sqrt{\sum_{i=1}^{n}\left(\frac{\partial_f}{\partial_{x_i}} * \sigma_{x_i}\right)^2} \tag{41}$$

With the *function* $\varphi = f(X)$ and $X = \left(x_1, x_2, \ldots, x_n\right)$ with the respective standard deviations $\sigma_{x_1}, \sigma_{x_2}, \ldots, \sigma_{x_n}$.

4.7. Transformation of coordinates

Cartesian coordinates (like ITRF-Coordinates), especially the z-values, are not representative for a comparison of different stations. Because they do not represent the actual height (by means of an orthogonal distance) above the earth surface, or a reference sphere at a specific location. However, this can be realized with an ellipsoidal coordinate system, whose coordinates are defined by ellipsoidal latitude φ [rad], ellipsoidal longitude λ [rad] and ellipsoidal altitude h [m] (see fig. 4).
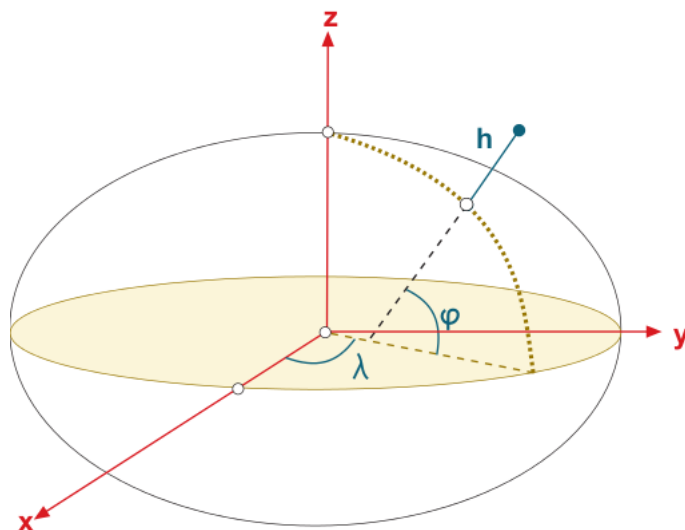
Figure 4: Illustration of ellipsoidal coordinates in a cartesian system. Source: *www.navipedia.net*, Jan. 2018

The following formulas allow an iterative transformation from global cartesian coordinates to ellipsoidal coordinates:

With the known ellipsoidal constants semi-major axis a and the numerical eccentricity e, as well as an apriori-value for φ_0 h, φ and λ can be determined iteratively through the following formulas [Bauer, 2011]:

$$\overline{N} = \frac{a}{\sqrt{1 - e^2 \sin \varphi_0{}^2}} \tag{42}$$

$$h = \frac{\sqrt{\overline{X^2} + \overline{Y^2}}}{\cos \varphi} - \overline{N} \tag{43}$$

$$\varphi = \arctan \frac{\overline{Z}}{\sqrt{\overline{X^2} + \overline{Y^2}}} \left(1 - e^2 \frac{\overline{N}}{\overline{N} + h} \right)^{-1} \tag{44}$$

$$\lambda = \arctan \frac{\overline{Y}}{\overline{X}} \tag{45}$$

Helmert Transformation (3D)

The three-dimensional Helmert Transform (also called "*Bursa-Wolf-Model*") is a 7-Parameter Transformation commonly used in Photogrammetry and Geodesy transforming point coordinates between two different cartesian coordinate systems. The transformation function (see eq. 46) describes the transformation between *system 1* represented through (x, y, z) and *system 2*, represented through (X, Y, Z):

$$\begin{pmatrix} X \\ Y \\ Z \end{pmatrix} = \begin{pmatrix} \delta x \\ \delta y \\ \delta z \end{pmatrix} + (1 + m) \cdot R(\alpha, \beta, \gamma) \begin{pmatrix} x \\ y \\ z \end{pmatrix} \tag{46}$$

The rotation matrix $R(\alpha, \beta, \gamma)$ is composed by three smaller matrices, describing the rotation around each axis:

$$R(\alpha, \beta, \gamma) = R_z(\gamma) \cdot R_y(\beta) \cdot R_x(\alpha) \tag{47}$$

whereas

$$\mathbf{R}_x(\alpha) = \begin{pmatrix} 1 & 0 & 0 \\ 0 & \cos\alpha & \sin\alpha \\ 0 & -\sin\alpha & \cos\alpha \end{pmatrix}$$

$$\mathbf{R}_y(\beta) = \begin{pmatrix} \cos\beta & 0 & -\sin\beta \\ 0 & 1 & 0 \\ \sin\beta & 0 & \cos\beta \end{pmatrix} \tag{48}$$

$$\mathbf{R}_x(\gamma) = \begin{pmatrix} \cos\gamma & \sin\gamma & 0 \\ -\sin\gamma & \cos\gamma & 0 \\ 0 & 0 & 1 \end{pmatrix}$$

With very small rotation angles α, β, γ, R can be simplified to

$$R(\alpha, \beta, \gamma) = \begin{pmatrix} 1 & \gamma & -\beta \\ -\gamma & 1 & \alpha \\ \beta & -\alpha & 1 \end{pmatrix} \tag{49}$$

Thus the 7 parameters describing the transformation are [Navratil, 2006]:

- δx, δy, δz translation vectors for the respective directions

- α_x, β_y, γ_z as rotation angles around the respective axis

- m as a scale-factor between the two systems

5. Data

For the analysis, data from May, 6th to May, 20th 2014 was processed. Both, VLBI and SLR data were preprocessed and saved in SINEX files which provided information about station coordinates, EOP and technique specific values, as well as stochastic information (see below in respective section). The available data is based on measurements at 17 VLBI stations and 30 SLR stations. At four locations, where VLBI as well as SLR measurements were recorded, so called local ties are available between the observing units. Local ties are very precise locally measured vectors between the two ground stations (VLBI and SLR) that build a link between the two reference systems.

Figure 5: Global distribution of VLBI and SLR stations. Source: www.maps.google.com

Figure 5 shows the locations of the observatories on a global map. It is obvious, and overall one of the biggest challenges, that their global distribution is not homogenous and the southern hemisphere is lacking space geodetic facilities (see tab. 2).

	South	North	Overall
VLBI	7 (42 %)	10 (58 %)	17
SLR	6 (20 %)	24 (80 %)	30
LT	2 (50 %)	2 (50 %)	4
Total	13 (28 %)	34 (72 %)	47

Table 2: Distribution of observatories in the southern and northern hemisphere.

5.1. VLBI

The VLBI-SINEX data was recorded and derived through the Continous VLBI Campaign 2014 (CONT14). The CONT-Campaigns are continous VLBI-Campaigns held in irregular intervals since 1994 including 17 stations distributed over the whole globe (10 in the northern hemisphere, 7 in the southern hemisphere, see tab. 2). According to the International VLBI Service Geodesy & Astronomy (IVS) the goal of CONT14 was to *"acquire state-of-the-art VLBI data over a time period of about two weeks to demonstrate the highest accuracy of which the current VLBI system is capable."* [IVS Website, 2014] The VLBI data is provided by the Bundesamt für Kartographie und Geodäsie (BKG) in SINEX 2.10 format. There are 15 CONT14-files including daily single session information about:

- A-priori and estimated values for
  - Station coordinates ($X_{VTRF2008A}$ [m], $Y_{VTRF2008A}$ [m], $Z_{VTRF2008A}$ [m])
  - Source coordinates (*right ascension*$_{ICRF2}$ [rad], *declination*$_{ICRF2}$ [rad])
  - EOP
    - Polar motion (X [mas], Y [mas])
    - Polar motion rates (X [mas/d], Y [mas/d])
    - UT1 [ms]
    - LOD [ms]
    - Nutation (X [mas], Y [mas])
- Right hand side vector n (decomposed)
- Normal equation matrix N (decomposed)
- Statistical information (Standard deviation, Variance factor)

In further graphs and illustrations the stations will be denoted by their ID codes, shown in the following table (3):

ID	Station	ID	Station	ID	Station
7382	BADARY	7298	KOKEE	7209	WESTFORD
7297	FORTLEZA	7243	MATERA	7224	WETTZELL
7378	HART15M	7331	NYALES20	7376	YARRA12M
7374	HOBART12	7213	ONSALA60	7386	YEBES40M
7242	HOBART26	7345	TSUKUB32	7381	ZELENCHK
7375	KATH12M	7377	WARK12M		

Table 3: Official IVS station identifier codes (VLBI)

5.2. SLR

Two different SLR datasets have been used. The first is from Agenzia Spaziale Italiana (ASI) with 15 daily single session files, containing data from the same time span as the VLBI (CONT14) files. The second one is from Bundesamt für Kartographie und Geodäsie (BKG) with 13 single session files of the same time period. Because of strong constraints and resulting biases in the ASI data (see chapter 6.2 and appendix A), the final calculations were executed with BKG data. As mentioned in the introduction to this chapter, and especially concerning SLR, the global station distribution is very inhomogenous (see fig. 5 and tab. 2). One reason for that is the strong dependency on the current meteorological conditions. Therefore, SLR investigations are commonly based on weekly data. However, for this thesis daily data was used.

They all contain information about
- A-priori and estimated values for
  - Station coordinates ($X_{SLRF2008}$ [m],$Y_{SLRF2008}$ [m],$Z_{SLRF2008}$ [m])
  - Range biases [m]
  - EOP
    - Polar motion (X [mas],Y [mas])
    - LOD [ms]
- Stochastic information
  - Covariance matrices (a-posteriori, constraint)
  - Variance factor

Table 4 shows the station codes for the SLR stations, which will be used as identifier in the following graphs and illustrations.

ID	Station	ID	Station	ID	Station
1868	Komsomolsk	7110	Monument	7820	Kunming
1873	Simeiz	7119	Haleakala	7821	Shanghai
1879	Altay	7124	Papeete	7825	Mount
1886	Arkhyz	7237	Changchun	7838	Simosato
1887	Baikonur	7249	Beijing	7839	Graz
1888	Svetloe	7359	Daedeok	7840	Herstmonce
1890	Badary	7403	Arequipa	7841	Potsdam
7080	Mcdonald	7406	San	7845	Grasse
7090	Yarragadee	7501	Hartebeest	7941	Matera
7105	Greenbelt	7810	Zimmerwald	8834	Wettzell

Table 4: Official ILRS station identifier codes (SLR)

5.3. Local ties

The local tie data consists of station coordinates and stochastic information determined through independent local geodetic surveys. They are as well provided in SINEX files and used as a connection between VLBI and SLR reference frames. Comparing the observatory locations of VLBI and SLR (fig. 5) shows that there are six co-location sites. From four of them information about the local ties was available:

- Wettzell (GER, 2014)

- Matera (ITA, 2009)

- Hartebeesthoek (ZAF, 2015)

- Yarragadee (AUS, 2013)

The SINEX files contain estimated station coordinates (X_{ITRF}, Y_{ITRF}, Z_{ITRF}) plus standard deviations for all, in this case VLBI and SLR, measurement units and respective covariance matrices resulting from the local terrestrial surveys.

Site ($Name$, ID_{VLBI}, ID_{SLR})	Coordinate differences (dx, dy, dz) [m]	length of LT-Vector [m]
Wettzell 7224, 8834	36.9755 50.1943 -45.8011	77.3589
Matera 7243, 7941	40.0952 64.4576 -76.1100	107.4948
Hartebeesthoek 7378, 7941	-89.6990 168.9004 4.0103	191.2834
Yarragadee 7376, 7090	111.5350 20.5332 -66.7900	131.6153

Table 5: Local ties at co-location site between VLBI and SLR observing units.

6. Methodology and Processing

The major part of data processing was executed with the mathematical programming software *MATLAB*. In a first step the preprocessed VLBI- and SLR-SINEX data were analyzed and brought into a common, or global, structure in order to execute the combination processes (eq. 25).

The general workflow consisted of

- Preparation of N and n (chapter 4.2 and 4.3).

- Stacking of N and n (chapter 4.4)

- Implementation of local ties (chapter 4.5)

- Datum definition (chapter 4.5)

- Inversion of the NEQ (chapter 4.1)

- Addition of residuals onto a priori values (eq. 17)

During the investigation different stacking- and constraining methods were applied and will be described in the following subchapters.

6.1. VLBI

As described in chapter 5.1 the VLBI data includes decomposed N-Matrices and right-hand-side-vectors n based on parameters refering to station coordinates, source coordinates and EOP. In a first step the rows and columns refering to source coordinates were cut. All files refered to the exact same parameters in the same order. Therefore, the original structure of the matrices could be kept and is shaped as follows:
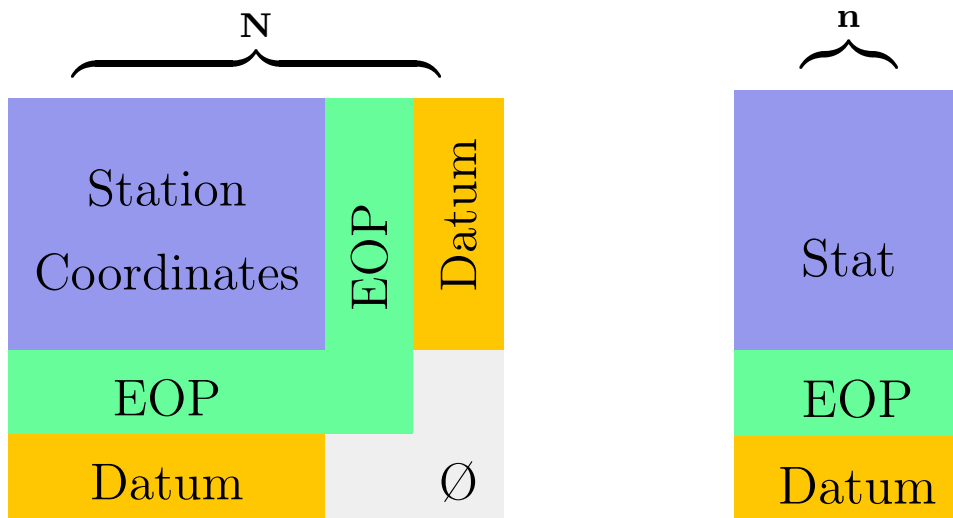
For the determination of the daily weighting factor (see tab. 6) equation 27 was applied. The session specific variance factor σ_{0i} was provided by the respective SINEX files and σ_0 was set to be the mean value of all fifteen (daily) variance factors. EOP-values, although representing the same parameters, were not stacked together, because of the temporal differences between the sessions. Thus, they were treated as individual parameters for each session (ref. to eq. 25).
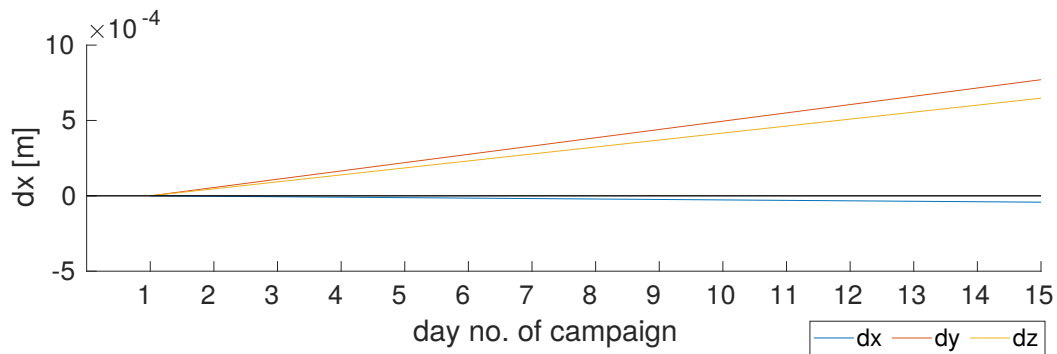
Figure 6: The a-priori coordinates are not stable for the CONT14 campaign. Here at Hartebeesthoek (ID 7378) station.

The geodetic datum was defined by a-priori coordinates of sixteen out of the seventeen CONT14 stations and applied according to equation 32. Only the observatory in Tsukuba, Japan, was not included as its coordinates were unstable due to an earthquake taking place in that area during the CONT14 time period [Vervaeck, Armand, 2014].

Daily VLBI Weighting Factors λ_i		
No. 1-5	**No. 6-10**	**No. 11-15**
1.0451	1.1779	1.1201
0.8902	0.9496	0.9418
1.0236	0.9119	0.9914
1.0431	0.9433	1.0525
0.9072	1.1503	0.9610

Table 6: λ_i as the quotient of day-specific variance factors and the mean variance factor of all 15 sessions.

Note that the daily a-priori values were not constant (see fig. 6). Therefore, the stacked normal equation matrix was constrained with the a-priori values of day 1.

Inverting the NEQ (eq. 16) delivered residuals for each a priori station coordinate.

This procedure was applied on every daily sessions data, as well as on the derived stacked data.

6.2. SLR

Other than for VLBI, there were no SLR normal equation matrices provided in the SINEX
files. Therefore a few preprocessing steps had to be executed.

In a first step, applying equation 23 and 24 on
the given covariance matrices yielded decom-
posed normal equation matrices. As noted in
chapter 5.2 the original SLR data included in-
formation about range biases. However, due
to singularities appearing during further calcu-
lations, corresponding rows and columns were
reduced following formulas described in chapter
4.2.

Daily SLR Weighting Factors λ_i		
No. 1-5	**No. 6-10**	**No. 11-13**
0.8683	1.3290	0.9370
0.8613	1.1423	0.8073
0.9118	1.1049	0.9107
1.0245	1.0931	
1.0348	1.2556	

Table 7: λ_i as the quotient of
day-specific variance factors and the
mean variance factor of all 13 SLR
sessions.

Afterwards, the matrices were restructured into
a global pattern (necessary for stacking; see eq.
25), as not every station provided data for every
session (see tab. 8).

The daily weighting factors λ_i were determined in the same way as for VLBI (eq. 27). σ_0,
as technique-specific variance factor, was determined as the mean value of all variance
factors σ_{0i} (see tab. 7).

The datum definition for the SLR solution was based on the station coordinates of all
appearing stations in the respective session.

For the sake of completeness, it should be mentioned that originally the investigations
and processings were started with SLR SINEX data from Agenzia Spaziale Italiana. This
would have had the advantage, that, like for VLBI, datasets for all 15 consecutive days
would have been available. However, the data appeared to have some stronger constraints
applied, which could not be decomposed. This led to relatively large and clearly biased
residuals. Some results can be seen in the appendix A.

6.3. Combination of VLBI and SLR NEQs

The inter-technique combination is based on stacked decomposed VLBI and SLR normal
equations. It is important to mention, that both datasets (VLBI and SLR) were recorded
within the same time frame. The combination of the (constraint free) normal equation
matrices was accomplished through the application of equation 28. The weighting factors
were chosen as $\lambda_j = 1/\sigma_{j0}^2$ with the technique-specific σ_{j0}^2 as the mean value of the daily

		Sessions (day of campaign)													No. of observ.
		1	**2**	**3**	**4**	**5**	**6**	**7**	**8**	**9**	**10**	**11**	**12**	**13**	
	1868											x	x	x	**3**
	1873			x	x	x	x	x	x				x	x	**8**
	1879	x	x	x	x	x	x	x	x	x	x	x	x	x	**13**
	1886						x	x	x	x	x	x	x	x	**8**
	1887	x	x	x	x	x	x	x	x	x	x	x	x	x	**13**
	1888	x	x	x	x	x	x	x	x	x		x	x	x	**12**
	1890						x	x	x	x	x	x			**6**
	7080	x	x	x	x	x	x	x	x	x	x	x	x	x	**13**
	7090	x	x	x	x	x	x	x	x	x	x	x	x	x	**13**
	7105	x	x	x	x	x	x	x					x	x	**9**
	7110	x	x	x	x	x	x	x	x	x	x	x	x	x	**13**
	7119		x	x	x	x	x	x	x	x	x	x	x	x	**12**
Station ID	**7124**	x								x	x	x	x	x	**6**
	7237	x	x	x	x	x	x	x	x	x	x	x	x	x	**13**
	7249	x	x	x	x	x	x	x	x	x	x	x	x	x	**13**
	7359	x	x	x	x	x	x	x	x	x	x	x	x	x	**13**
	7403	x	x	x	x	x	x	x	x	x	x	x	x	x	**13**
	7406	x	x	x	x	x	x	x	x	x	x	x	x	x	**13**
	7501	x	x	x	x	x	x	x	x	x	x	x	x	x	**13**
	7810	x	x	x	x	x	x	x	x	x	x	x	x	x	**13**
	7820					x	x	x	x	x	x	x	x	x	**9**
	7821	x	x	x	x	x	x	x							**7**
	7825	x	x	x	x	x	x								**6**
	7838	x	x	x	x	x	x	x	x	x	x	x	x	x	**13**
	7839	x	x	x	x	x	x	x	x	x	x	x	x	x	**13**
	7840	x	x	x	x	x	x	x	x	x	x	x	x	x	**13**
	7841	x	x	x	x	x	x	x	x			x	x	x	**11**
	7845	x	x	x	x	x	x	x	x	x	x	x	x	x	**13**
	7941	x	x	x	x	x	x	x	x	x	x				**10**
	8834	x	x	x	x	x	x	x	x	x	x	x	x	x	**13**
No. of obs. stations		**24**	**24**	**25**	**25**	**26**	**28**	**27**	**25**	**24**	**23**	**25**	**26**	**26**	

Table 8: SLR stations and their measurement schedules.

σ_{j0i}^2 (j denoting the space geodetic technique - in this case VLBI (v) or SLR (s) - and i denoting the session index of the respective campaign).

Different approaches were used for the definition of the geodetic datum of the combined solution, varying in the amount and type of stations, whose *a-priori* coordinates were taken into account:

λ_{v0}	λ_{s0}
0.9928	0.9789

Table 9:
Weighting factors
for the combined
solution.

- only VLBI station coordinates

- only SLR station coordinates

- VLBI and SLR station coordinates

- only station coordinates of co-location sites (ITRF)

In addition, solutions were calculated with the scale considered as (a) a constrained parameter or (b) an independent parameter (compare eq. 30 and 31). Additionally local ties were introduced as connecting link between the two space geodetic techniques' systems. They were added as conditions describing relative constraints between parameters, represented through the locally measured tie vectors at co-location sites (see chapter 4.5). The distance (vector) between the two measuring units is represented by the following conditional equation.

$$\phi(X_V, Y_S) = d_{vs}$$

$$X_V = \begin{pmatrix} x_V \\ y_V \\ z_V \end{pmatrix} \text{ and } X_S = \begin{pmatrix} x_S \\ y_S \\ z_S \end{pmatrix} \tag{50}$$

$$d_{vs} = \sqrt{(x_{v0} - x_{s0})^2 + (y_{v0} - y_{s0})^2 + (z_{v0} - z_{s0})^2}$$

or split up into the three components:

$$d_{x_{vs}} = x_{v0} - x_{s0}$$
$$d_{y_{vs}} = y_{v0} - y_{s0} \tag{51}$$
$$d_{z_{vs}} = z_{v0} - z_{s0}$$

According to chapter 4.5 the B-Matrix was obtained through the derivation of the conditional equation with respect to the parameters, which resulted in:

$$B = \begin{pmatrix} \frac{d\Phi}{dx_V} & \frac{d\Phi}{dy_V} & \frac{d\Phi}{dz_V} & \frac{d\Phi}{dx_S} & \frac{d\Phi}{dy_S} & \frac{d\Phi}{dz_S} \end{pmatrix} \tag{52}$$

$$B_{d_{vs}} = \begin{pmatrix} \frac{x_v-x_s}{d_{vs}} & \frac{y_v-y_s}{d_{vs}} & \frac{z_v-z_s}{d_{vs}} & -\frac{x_v-x_s}{d_{vs}} & -\frac{y_v-y_s}{d_{vs}} & -\frac{z_v-z_s}{d_{vs}} \end{pmatrix}$$

in case of the use of equation 50, or

$$B_{\overline{vs}} = \begin{pmatrix} 1 & 0 & 0 & -1 & 0 & 0 \\ 0 & 1 & 0 & 0 & -1 & 0 \\ 0 & 0 & 1 & 0 & 0 & -1 \end{pmatrix}$$

in case of the use of equation 51.

Hence, the structure of the complete NEQ-System is illustrated below.
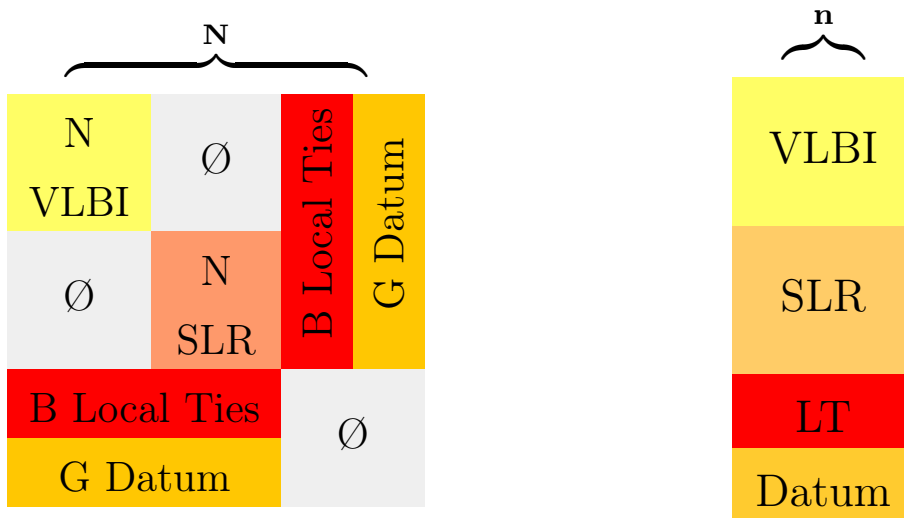
The inversion of this system (according to equation 16) yields residuals for both, VLBI and SLR station coordinates, which are illustrated in chapter 7. The blocks "*N VLBI*" and "*N SLR*" are structured as described in chapter 6.1. However the rows and columns of the technique-specific normal equations representing the datum are left out, because the global geodetic datum is defined by the combined solution as described previously.

Local tie selection

Data sets from four different co-location sites were available. As they did not include actual values for the local tie vector, but coordinates for the stations (including respec-

tive standard deviations), the length of the vectors had, in a first step, to be determined through the differences between the coordinates. Applying the error propagation law, standard deviations could be derived to evaluate the vectors (see tab. 10).

Station	LT [dX, dx, dy, dz]		StD [dX, dx, dy, dz]	
1 Matera dX [m]	107, 49		0, 0014	
dx [m]		40.10		0.0014
dy [m]		64.46		0.0006
dz [m]		-76.11		0.0017
2 Wettzell dX [m]	77.36		0.0005	
dx [m]		36.98		0.0005
dy [m]		50.19		0.0004
dz [m]		-45.80		0.0006
3 Hartrao dX [m]	191.28		0.0038	
dx [m]		-89.70		0.0034
dy [m]		168.90		0.0039
dz [m]		4.01		0.0085
4 Yarragadee dX [m]	131.62		0.0005	
dx [m]		111.53		0.0005
dy [m]		20.53		0.0005
dz [m]		-66.79		0.0004

Table 10: Local ties - distances and standard deviations

As a rule of thumb a maximum standard deviation of 5 mm was chosen. All four local ties passed this criteria and were considered as valuable contribution to the adjustment computations. Practically, the selection with respect to which and how many local ties were added to the NEQ system was optional. The differences are shown in chapter 7.

7. Results

This section presents the result of the data processing described in chapter 6. The first two subchapters show the intra-technique solutions and the third one the combined (local ties included) solutions and their variations.

7.1. VLBI
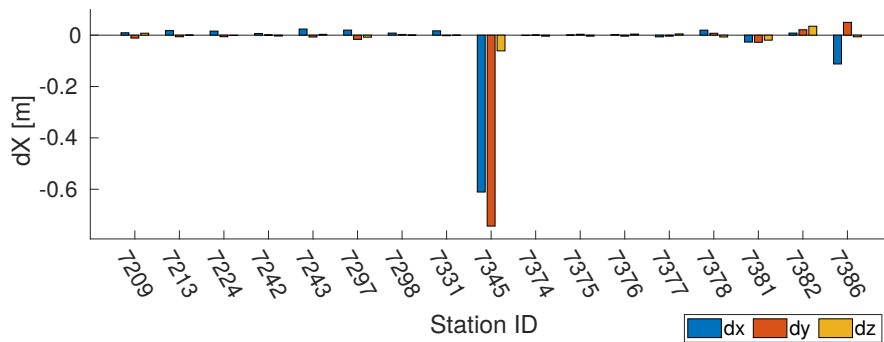
Figure 7: Residuals (dX) derived from the combined (stacked) VLBI NEQ

Figure 7 presents the resulting residuals for each CONT14 participating station, derived from the inversion of the intra-technique stacked *NEQ*. As mentioned in chapter 5 an earthquake took place close to the Tsukuba (ID 7345) observatory, which explains the relatively large residuals (more than half a meter in x- and y-direction). For a better illustration, figure 8 shows the residuals for each station, except Tsukuba, and table 11 presents its statistical charactercistics. Note that they are derived from the respective absolute values and are within the *cm*-range.
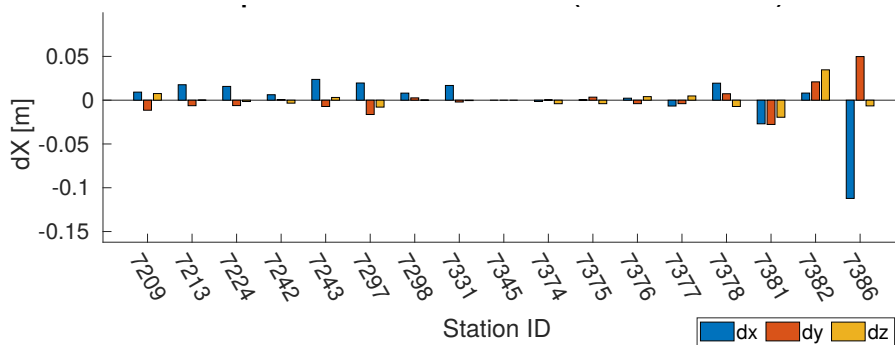
Figure 8: Residuals (dX) derived from the combined (stacked) VLBI NEQ, Tsukuba (7345) excluded.

	dX	dx	dy	dz
mean [mm]	39.01	53.27	53.76	10.01
mean OF [mm]	11.96	18.42	10.65	6.81
std [mm]	135.08	151.45	181.05	18.39
std OF [mm]	21.64	32.44	16.98	11.23

Table 11: Characteristics for the solution of the intra-technique VLBI combination. "OF" indicates, that Tsukuba was excluded.

Solutions for individual days yield generally similar results as the stacked solution. Taking a look at the developement of residuals at one station over the course of the measurement campaign does not indicate any significant trend within the data. Nevertheless the time span would be too short for a plausible evaluation. The following figures (fig. 9) show the time-dependence of residuals (upper graphic - daily residuals) at Hartebesteok observatory and its variations with respect to day 1 (lower graphic). The average variations are characterized by the parameters in table 12.
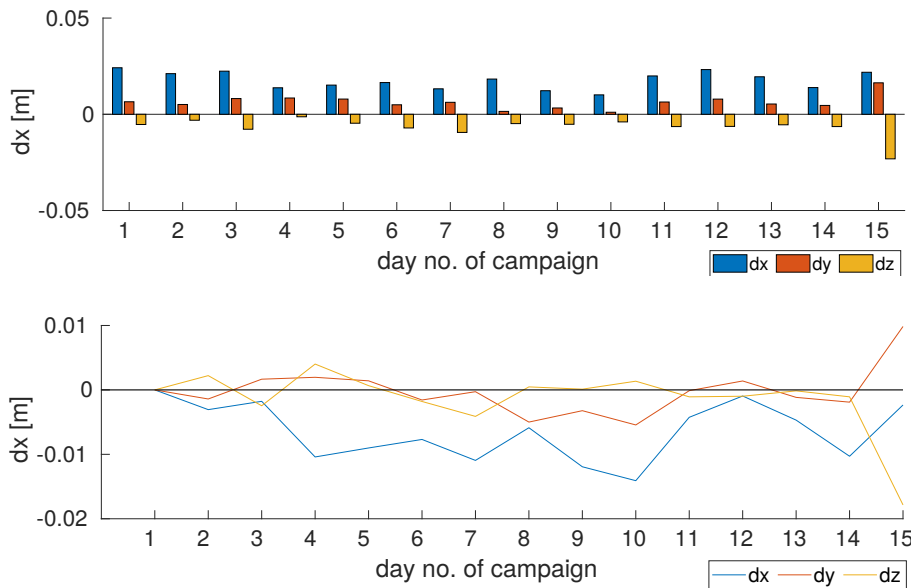
Figure 9: Hartebeesthoek VLBI Station (ID 7378) during the CONT14 campaign.

Note that the variation over time per day (ddX) is close to a factor 10 smaller than the actual residuals and stays within the low *cm*-range.

	ddX	ddx	ddy	ddz
mean [mm]	4.61	5.32	3.63	4.87
std [mm]	6.22	7.02	4.96	6.49

Table 12: Charateristics describing the development of the residuals over the course of the measurement campaign gathered from all VLBI stations. The mean values are refered to the absolute residual-lengths.

7.2. SLR

The residuals of the stacked SLR-solution are presented in figure 10. Note that not every station provided data for each day. This has an impact on the estimation and the resulting residuals. The largest estimations were found at stations where no daily data was available (see tab. 8).
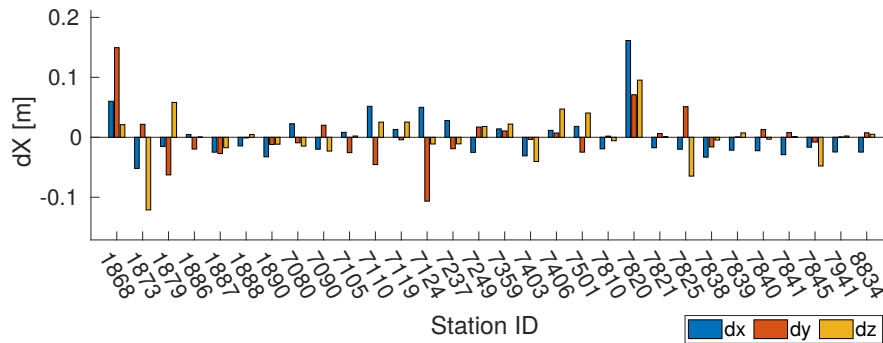
Figure 10: Residuals (dX) derived from the combined (stacked) SLR NEQ

Excluding the data from Komsomolsk (ID 1868, 3 observations), Simeiz (ID 1873, 8 obs.), Papeete (ID 7124, 6 obs.) and Kunming (ID 7820, 9 obs.) reduces the mean residuals by more than 7 mm (tab. 13).

	dX	dx	dy	dz
mean [mm]	26.78	29.57	25.69	25.09
mean OF[mm]	19.10	21.68	16.23	19.38
std [mm]	40.36	41.25	42.49	38.62
std OF [mm]	24.19	22.45	22.31	27.50

Table 13: Characteristics of the intra-technique SLR (stack) solution. The with "OF" denoted values are based on a reduced set of stations (1868, 1873, 7120 and 7124 are excluded).

Again, the residual-variation over the time of the measurment campaign does not suggest a significant bias or trend. However, a well-based statement about that would require

more data to be investigated. Hence, taking a look at the development of residuals at one station shows variations within the *cm*-range. Missing bars in some graphs indicate that there was no data available for a certain day at the respective station.
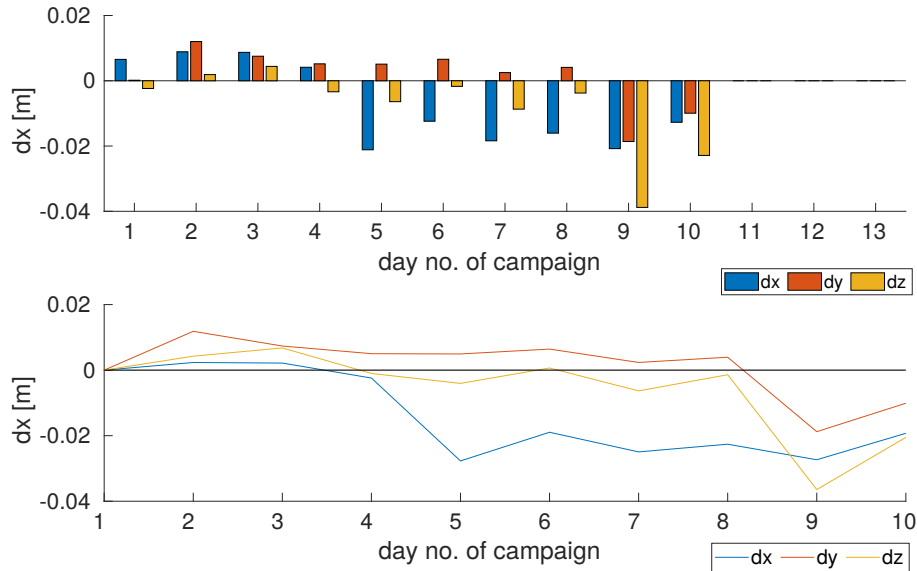
Figure 11: Hartebeesthoek SLR Station (ID 7941) during the CONT14 campaign time frame. Note that there is no data available for day 11, 12 and 13.

Compared to VLBI, the SLR results are less stable (see fig. 11). The daily variations are significantly larger and almost of the same size as their actual values.

	ddX	**ddx**	**ddy**	**ddz**
mean [mm]	22.79	23.67	25.27	19.45
std [mm]	36.32	36.98	40.50	30.95

Table 14: Statistical values of the development of the residuals gathered from all stations. (compare fig. 11) for Hartebeesthoek. *ddX* stands for the differencial residual w.r.t. day 1.

7.3. Combination of VLBI and SLR

Depending on the selected option related to the definition of datum and the selection of local ties (see chap. 6.3), different results were derived for a combined solution. Some representative results are presented in this section and their differences are highlighted. The illustrations are always based on the same structure. The upper plot shows the residuals, derived from the NEQ-Inversion; the lower plot shows the difference to the

solution of the intra-technique combination (chap. 7.1 and 7.2). The small coloured squares below the abscissa mark co-location sites. Further, statistical characterization of transformation parameters, which describe effects on the station coordinates are displayed in tables. Note, that each table includes values for VLBI-Stations and SLR-Stations (grey background color) and the adding "OF" stands for "outlier free", which means that the most off-sized values (stations - e.g. Tsukuba VLBI) are excluded from statistical analysis. The *Helmert Parameters* are estimated through the *Bursa-Wolf Model* (see chap. 4.7) and describe a transformation from the technique specific solution towards the combined solution. The rotation values are transformed to lengths ($[mm]$) and scaled to their impact on the earth surface ($[rad] \cdot 6371000$ - earth radius in $[m]$). The value representing the scale is the length-difference of a distance of 6371 km (earth radius) between the intra- and inter-technique solutions in $[mm]$.

Another characteristic value was chosen to be the mean ΔLT, refering to the mean value of the differences between the lengths of the original local ties (from the LT-SINEX files) and their lengths calculated from the estimated station coordinates after the application of the adjustment computations. Those differences appear because, the station coordinates are provided in different reference systems. Note, that the provided data always refers to the technique-specific reference frames and the local ties are given in the ITRF. Thus, chosing a technique-specific datum makes it theoretically impossible to satisfy the introduced condition exactly and yields local tie variations ($\Delta LT \neq 0$). But replacing the datum-giving a priori coordinates at co-location sites with ITRF coordinates yields compliance of the local tie condition, which results in $\Delta LT = 0$ mm.

6 representative combination configurations are illustrated and described in detail. Table 15 gives an overview of the following 6 options.

Option	Local ties	Datum	Main Statement
# **1**	4	VLBI	homogenous distribution, V shift
# **2**	4	SLR	intermediate distribution, S shift
# **3**	4	VLBI, SLR	weak distr., 2 systems in datum do not match
# **4**	3	VLBI	minimize ΔLT
# **5**	2	VLBI	minimize ΔLT
# **6**	4	Co-Loc. Sites (ITRF)	homogenous distribution, $\Delta LT = 0$

Table 15: Configuration options, whose results will be presented in detail below.

Option 1:

Datum definition: VLBI

Local ties: all 4

Selecting only VLBI station coordinates (except Tsukuba observatory) for the combined datum definition yields the most stable results in terms of relatively small and homogenously distributed residuals (see fig. 12, 13 and 14).
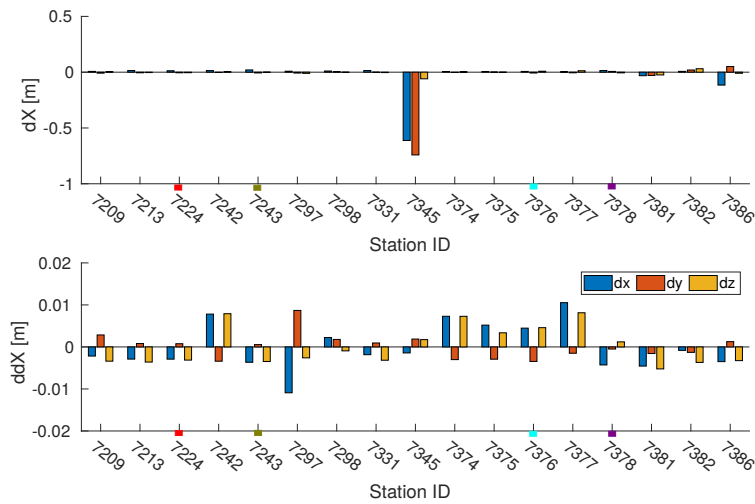
Figure 12: Residuals and differential residuals for VLBI stations. Datum definition: VLBI

For a better resolution the same results are plotted with an expanded scale without the large residuals at Tsukuba Observatory (7345) - "OF".
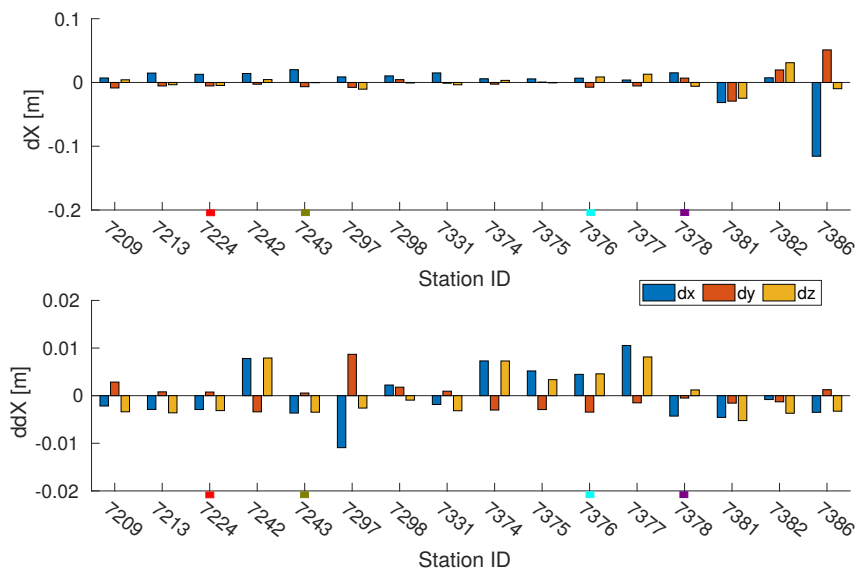
Figure 13: Residuals and differential residuals; excl. Tsukuba. Datum definition: VLBI
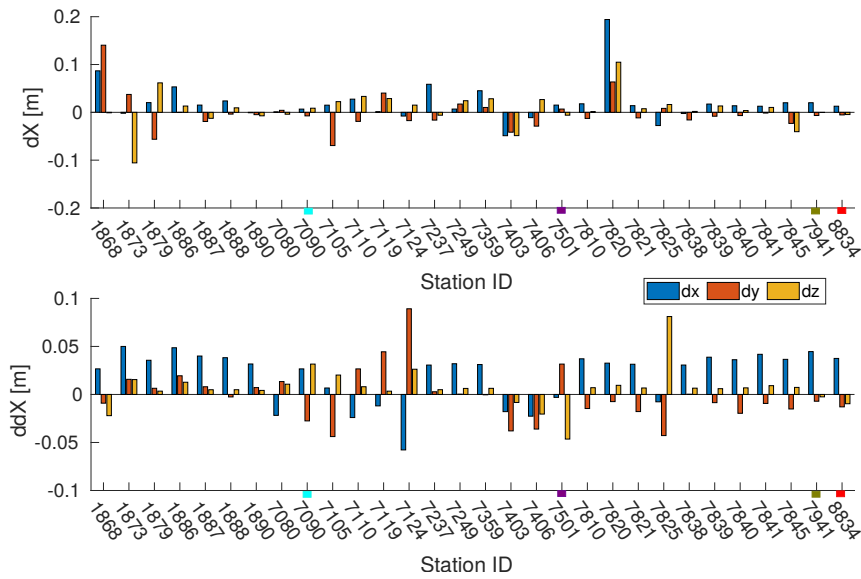
Figure 14: Residuals and differential residuals for SLR stations. Datum definition: VLBI

The residuals for VLBI stations are mostly in the *mm*-range (median of 7 *mm*), whereas the SLR-residuals are within the *cm*-range (see tab. 16). The difference with respect to the intra-technique solutions indicates a shift towards the VLBI network, as the corresponding residual differences are clearly smaller than the respective residuals. In contrast, the SLR differences are larger than the residuals. This is confirmed by the 7 Helmert parameters (see tab. 19). The differences in scale show that the VLBI system is larger than the SLR system. They differ by a factor of 1.7 *ppb*. The mean variation of the local ties is 6 *mm* ($\Delta LT = 6.18$ *mm*).

VLBI SLR	dX	dx	dy	dz
mean [mm]	39.25	53.34	53.33	11.09
	24.13	26.66	23.48	22.26
mean OF [mm]	12.26	18.40	10.32	8.07
	17.73	19.15	17.15	16.90
median [mm]	7.32	12.82	6.64	4.65
	14.48	15.15	14.32	12.86
std [mm]	135.04	151.88	180.59	18.50
	38.50	41.35	37.35	34.63
std OF [mm]	21.95	32.89	16.84	11.98
	23.70	21.96	21.74	21.87

Table 16: Description of the residuals derived through combined solution, including 4 local ties and defining the global datum with VLBI stations. Stations 7345 (VLBI) and 1868, 1873, 7820 (SLR) are excluded for the "OF-Calculations".

	VLBI	dX	dx	dy	dz
	SLR				
	RMSE [mm]	4.35	5.36	2.89	4.43
		27.56	33.51	26.79	20.93
Helmert Parameters	Translation [mm]		0.08	1.38	1.61
			5.71	-2.45	5.74
	Rotation [mm] (alpha. beta. gamma)		0.06	-0.0641	0.1038
			2.7696	-22.7693	22.5482
	Scale [mm]	-6.70			
		5.82			

Table 17: Description of the residual differences between the intra- and inter-technique solutions. (Inter-technique solution derived through the combination including 4 local ties and defining the global datum with VLBI stations.

Option 2:

Datum definition: SLR

Local ties: all 4

Defining the global datum only over SLR station coordinates yields reversed results compared to *Option 1* and the relation between VLBI and SLR residuals above. The absolute values are larger than those derived from the "VLBI-constraining". Note, that the VLBI residuals, and in order also their differences to the VLBI only solution, are within the *dm*-range.
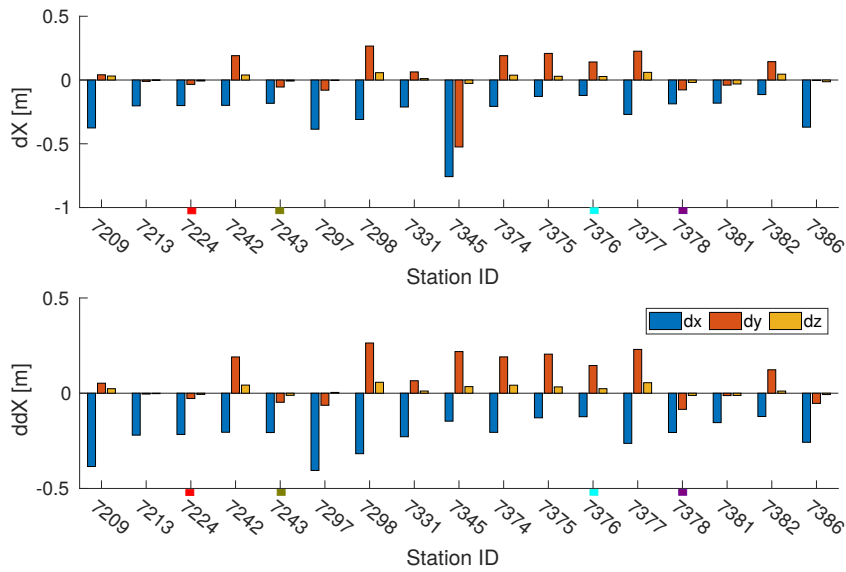
Figure 15: Residuals and differential residuals for VLBI stations. Datum definition: SLR
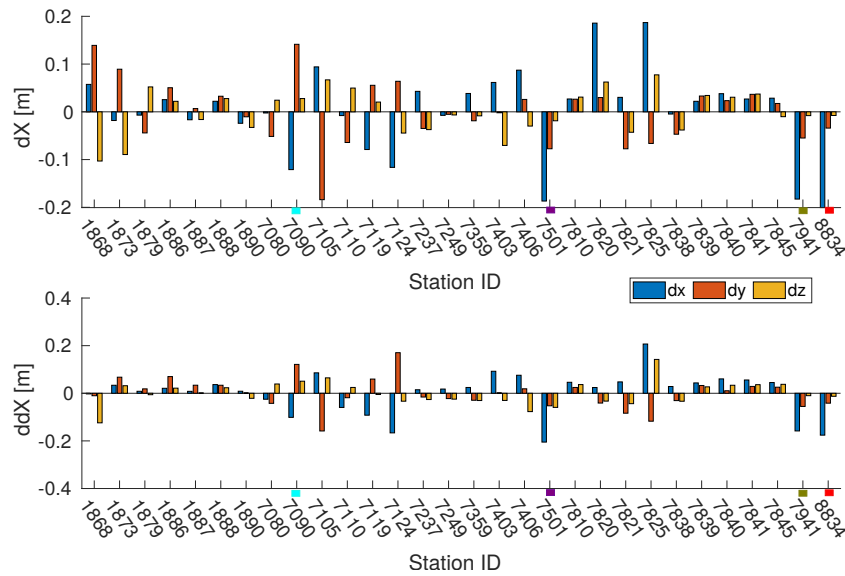
Figure 16: Residuals and differential residuals for SLR stations. Datum definition: SLR

Furthermore the values for the mean and median are closer, than in the VLBI-constraining. This indicates a more homogenous distribution of the residuals. Again the transformation parameters for the "datum-giving-technique" (here SLR) are smaller than for the "adapted" (here VLBI) one. As well, the scale parameters indicate, that the technique-specific VLBI system is larger than the SLR system. However, the estimated difference is smaller than in *Option 1*. The local tie variation is almost identical to *Option 1* with $\Delta LT = -6.18\,mm$. This is an interesting result and will be discussed later in more detail.

VLBI SLR	dX	dx	dy	dz
mean [mm]	140.25	259.00	135.18	26.57
	51.35	64.97	51.47	37.59
mean OF [mm]	121.75	227.84	110.83	26.57
	47.49	62.51	47.63	32.33
median [mm]	79.71	202.47	79.71	27.79
	34.56	34.14	40.43	31.76
std [mm]	193.63	154.62	186.06	29.60
	70.14	92.27	67.14	45.56
std OF [mm]	157.51	88.82	120.35	28.65
	65.90	89.20	62.03	37.75

Table 18: Description of estimated residuals dX. 4 local ties included; datum defined with SLR stations.

		VLBI SLR	dX	dx	dy	dz
		RMSE [mm]	160.72	237.36	142.55	28.83
			69.00	88.27	64.02	48.66
Helmert Parameters		Translation [mm]		-268.23	84.81	23.22
				0.10	0.28	0.72
		Rotation [mm] (alpha. beta. gamma)		19.05	-34.28	198.05
				0.00	0.00	0.00
		Scale [mm]	-6.73			
			-1,63			

Table 19: Description of the difference between residuals derived through intra-technique combination and inter-technique combination. The inter-technique solution is based on a SLR defined datum. 4 local ties included.

Option 3:

Datum definition: VLBI and SLR

Local ties: all 4

For completion and as an example for "extreme distortions", defining the global datum with the majority of both, VLBI and SLR, stations (in this case all except Tsukuba VLBI) delivers residuals that are unexpectedly large. The residuals range even up to m-dimensions but are proportionally evened out. Illustrations are added in appendix A. However, this configuration is not meant to proceed as the a priori coordinates refer to

different systems.

It is interesting to see that again ΔLT has an approximated value of $-6.18\ mm$ (as in *Option 1* and *Option 2*). This results from the fact, that the estimated residuals at the co-location sites have the same values for the VLBI and SLR coordinates (their calculated differences are below the measurement accuracies).

Further approaches, concerning the local tie selection and their implementation were investigated. Performing the calulations under stepwise slightly different configurations (see tab. 15, different configuration-options are described in chapter 4) adjusts the results towards the already described solutions. Hence, for *Option 3* adding the scale to the datum definition (see eq. 30) reduces the dimensions by a factor 10 to a *dm*-range. Further, introducing the local ties only one-dimensional (see eq. 50-52) adjusts the residuals even more to the single techniques constrained ones.

Taking a closer look at the local ties reveals differences between the station coordinates of the SINEX files. This is due to the fact that they all refer to different coordinates systems (VTRF, SLRF, ITRF). And although only the coodinate differences (lengths) are used for the adjustment calculations, this can be the reason for varying residuals. Table 20 shows the coordinate variations between the respective underlying systems. The different patterns at the co-location sites indicate different scales, which are not considered in the calculations and therefore can cause length-differences in the estimations. Additionally, the homogenous datum definition of inhomogenous station distributions (here w.r.t. the weight relations between VLBI and SLR) can cause distortions.

Co-Location Site		dX [mm]	dx [mm]	dy [mm]	dz [mm]
Matera	7243	525.7	323.1	-327.7	-254.1
	7941	527.6	318.4	-335.2	-254.1
	delta	**-1.9**	4.7	7.4	0.1
Wettzell	7224	43.9	24.9	-28.4	-22.2
	8834	52	17.8	-35.7	-33.3
	delta	**-8.1**	7.2	7.3	11.1
Hartebeesthoek	7378	29.1	-26.6	11.9	-0.3
	7501	24.6	-23.9	1.5	5.4
	delta	**4.6**	-2.7	10.3	-5.8
Yarragadee	7376	264	169.7	-41.2	-198
	7090	264.4	183.2	-36.6	-187.1
	delta	**-0.5**	-13.6	-4.6	-10.9

Table 20: The differences between the co-location site station coordinates from the technique-specific SINEX files and the local tie SINEX file are within the *mm*-range.

Several different local tie selections were investigated. Depending on how many and which local ties were implemented in the NEQ-System the "local tie difference" ΔLT could slightly be reduced:

Option 4:

Datum: VLBI
Local ties: Matera, Wettzell, Yarragadee (3)
$\Delta LT = -4.82 \ mm$
Chosing only three co-location sites (Matera, Wettzell, Yarragadee) does not have a significant impact on the overall residual statistics. Though, it decreases the mean ΔLT to $-4.82 \ mm$.

Option 5:

Datum: VLBI
Local ties: Matera, Wettzell (2)
$\Delta LT = -3.89 \ mm$
Similar to *Option 4*, but connecting the two techniques only via two local ties (Matera, Wettzell), does not yield significant changes within the statistics neither, but minimizes

the mean ΔLT even further to $-3.89\ mm$.

Varying the number of implemented local ties does not have a significant influence on the estimated scale differences, which in this case are between 1.7 and 1.9 *ppb*.

Further approaches, implementing the local ties only as a one-dimensional length of the vector (see chapter 6.3), or implementing scale to the datum definition were examined. A course summary and comparison of the results is presented in the following table 21.

		Datum			**+ Scale**			**1D LT impl.**		
		V	S	V, S	V	S	V, S	V	S	V, S
VLBI	dX	1 cm	1 dm	m	1 cm	1 dm	3 dm	1 cm	1 dm	7 cm
	ddX	4 mm	1 dm	m	1 mm	1 dm	3 dm	1 mm	1 dm	8 cm
	Scale	-6 mm	-7 mm	1 mm	0	-7 mm	-7 mm	0	7 mm	-7 mm
SLR	dX	2 cm	5 cm	m	2 cm	5 cm	6 dm	4 cm	2 cm	7 cm
	ddX	3 cm	-1 cm	m	3 cm	7 cm	9 dm	4 cm	3 mm	7 cm
	Scale	6 mm	1 mm	2 dm	6 mm	0	-4 cm	-7 mm	0	2 mm

Table 21: Comparison of different combination approaches. *V* stands for the VLBI-, *S* for SLR stations. All values are approximated mean values. *dX* stands for residuals, *ddX* for the residual differences w.r.t. intra-technique solutions. And *Scale* denotes the change of a distance of the earth radius ($6371km$) derived through a 7-Parameter Helmert transform between intra- and inter-combination solutions.

Figuring, that the presented results are not optimal and especially for the understanding of the ΔLT, a further definition of datum was implemented. Only co-location sites (VLBI and SLR) were considered as datum stations. And instead of constraining the system with the respective a priori values, ITRF coordinates, provided in the LT-SINEX files were taken into account.

Option 6:

Datum: co-location sites only - local tie frame (ITRF)
Local ties: all 4
$\Delta LT = 0\ mm$
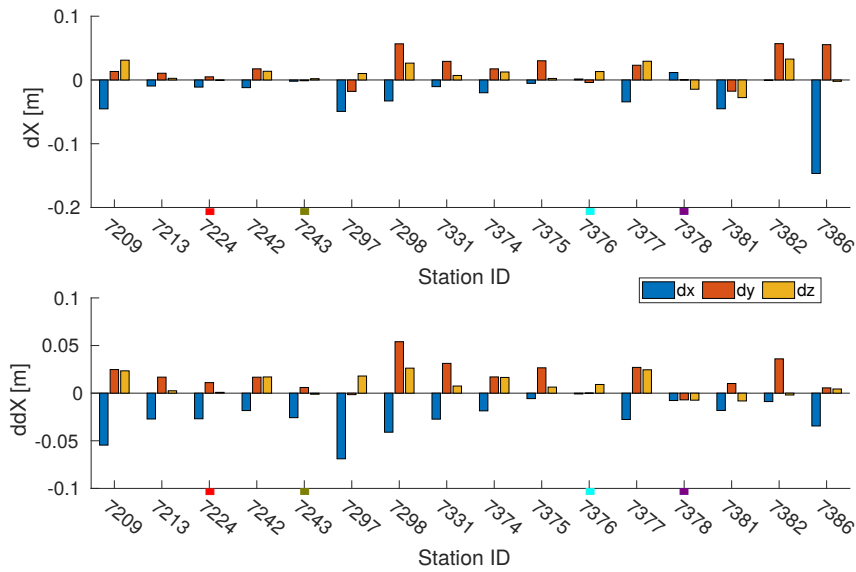
Figure 17: VLBI Residuals and differential residuals; only *Co-location sites* for datum definition
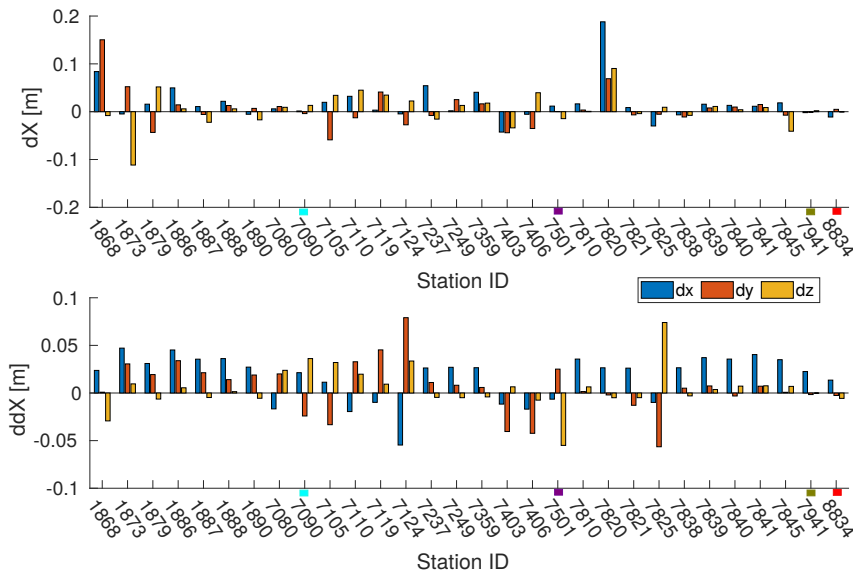
Figure 18: SLR Residuals and differential residuals; only *Co-location sites* for datum definition

The plots (fig. 17 and 18) and statistics (*Tab.* 22 and 23) are similar to *Option 1*. But, the main difference is, that with $\Delta LT = 0$ the condition for the preservation of the local ties is complied.

VLBI **SLR**	dX	dx	dy	dz
mean [mm]	46.91	62.53	61.71	16.49
	23.82	24.56	23.72	23.17
mean OF [mm]	21.29	27.38	22.25	14.25
	17.10	17.05	16.30	17.97
median [mm]	14.55	12.04	17.59	13.18
	13.01	12.45	11.92	13.86
std [mm]	133.18	149.73	173.81	21.76
	37.79	40.41	38.27	34.45
std OF [mm]	32.61	37.18	24.04	16.48
	22.43	21.03	22.34	22.63

Table 22: Description of estimated residuals dX. Datum definition: *Co-Location sites (ITRF)*

	VLBI **SLR**	dX	dx	dy	dz
	RMSE [mm]	24.15	30.30	25.43	13.59
		26.44	29.24	27.53	22.02
Helmert Parameters	Translation [mm]		4.44	-1.73	7.01
			-32.53	16.53	14.36
	Rotation [mm] (alpha. beta. gamma)		17.28	-21.38	17.08
			21.43	-6.95	32.17
	Scale [mm]	-6.47			
		4.47			

Table 23: Description of the difference between residuals derived through intra-technique combination and inter-technique combination. Datum definition: Co-location sites (ITRF)

Besides the difference in ΔLT, *Option 6* is quite similar to *Option 1*. However, the residuals appear to be slightly larger, but are distributed even more homogenously between VLBI- and SLR stations.

Taking a look at the variations of scale of the combined solutions w.r.t. the technique-specific solutions points differences between the two reference systems out. A distance of 6371 *km* (approximated earth radius) in the combined system is up to 7 *mm* shorter than in the VLBI system, but, depending on the combination configuration, a few millimeters longer than in the SLR system. Thus, based on the investigation of the two-week CONT14 data, it can be stated, that the VLBI system has larger scale than the SLR system. The

relative difference in scale between the two systems is (depending on the configuration) about 1.7 *ppb*.

8. Discussion

Residuals for VLBI and SLR a priori coordinates were derived, based on measurements during a two week time span in May 2014 (CONT14). They were estimated by combining data on the level of normal equations. Residuals were calculated separately for SLR and VLBI measurements, as well as for combinations of the two techniques. Different combination configurations (w.r.t. to the definition of datum and the implementation of local ties) yielded different results (see chapter 7). This provided insights on technique specific reference systems and their interaction concerning the generation of a Terrestrial Reference Frame (TRF).

Summarizing the results can be stated that the VLBI residuals are more stable and are distributed more homogenously (apart from Tsukuba) than the SLR residuals (see chapter 7.1 and 7.2). This has also an impact on the combined solutions, where the VLBI stations appear to have a stronger influence as datum giving parameters. Thus, the combined system is considered to fit best, if the global geodetic datum is defined by VLBI stations and the SLR stations are subsequently adjusted (*Option 1*). This approach yields an average residual size of about 1.5 *cm*. However, results vary within and between the respective techniques. One reason for the bigger impact of the VLBI sites is the fact that all 17 stations provided data for all 15 days of the campaign. In contrast there were 30 SLR stations, but not all provided the same amount of data.

Overall it was shown, that the definition of datum has a significant impact on the estimation of residuals. In particular this has to be considered for the combination of data from different reference systems. All datum defining parameters should come from the same reference system. There are two options for the scale parameter: It can be fixed within the datum (independent variable) or estimated (dependent variable). The choice depends on the desired parameters of interest. As, in this thesis, possible scale differences were investigated, it was, for the final results, not fixed within the datum. Comparing the two individual systems (VLBI and SLR) and the combined system it has been shown, that the scale of the VLBI system is larger than of the SLR system. They differ by, depending on the chosen configuration, about 1.7 *ppb* or have a difference in length of the approximated earth radius of 6371 *km* of about 1 *cm*. This confirms the differences between the two ITRF-scale-defining techniques mentioned in Altamimi et al. [2016], derived by the combination of solution approach (around 1.3 *ppb*).

To conclude it should be mentioned that the provided data from the 15 day time span might be too limited for well-founded statements. Hence, further research is needed for a

confirmation of the findings based on more data. Therefore data from different providers (processing centers), or covering longer time spans could be investigated, as possible long-term influences could not be considered in this thesis. Moreover the implementation of global ties (connecting the space geodetic techniques also via EOPs) can yield further insights.

A. Appendix

ad **Data/Processing:**

As mentioned in chapter 6, originally the project was started with SLR data provided from Agenzia Spaziale Italiana (ASI). But due to unexpeceted large and apparently biased residuals, different data (preprocessed at BKG) was investigated. Figure 19a shows the daily biased and large residuals at one station (Wettzell) and figure 19b shows the residuals derived from the data of day 1 (May, 1th, 2014). The advantage of the ASI data would have been, that SINEX files from all 15 campaign days would have been available.
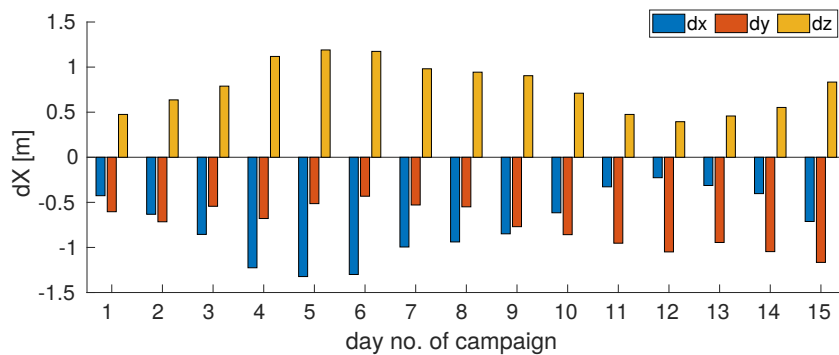
(a) Daily residuals derived from ASI data at Wettzell SLR observatory.
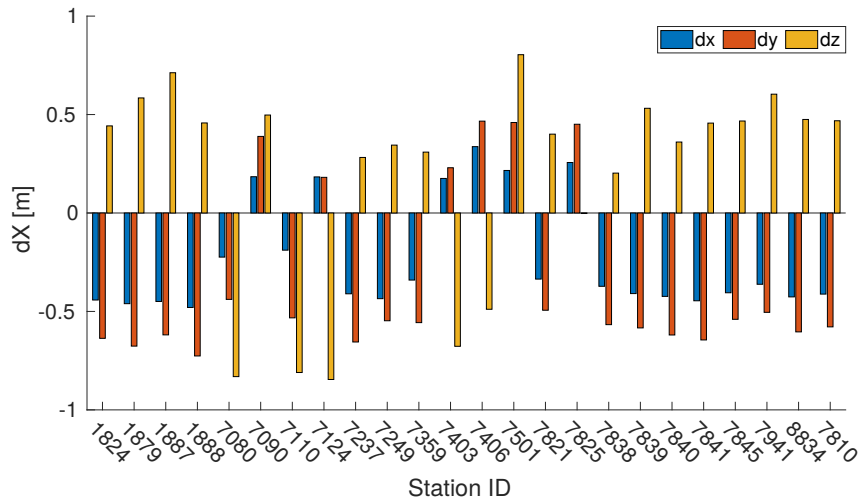
(b) Residuals derived from ASI data for day 1 of the measurement camapaign.

Figure 19: Residuals derived from ASI data, which was not continued to be used, nor was included in the inter-technique combinations.

Nevertheless those results were confirmed through a comparison to estimated solutions within the SINEX files, where the same pattern appeared. On request, the provider confirmed the noted effects and advised against the use of these datasets.

Analogue to the presented development of the available *a-priori* VLBI-coordinates (fig. 6), figure 20 shows the available a priori coordinates of Wettzell SLR station during the campaign:
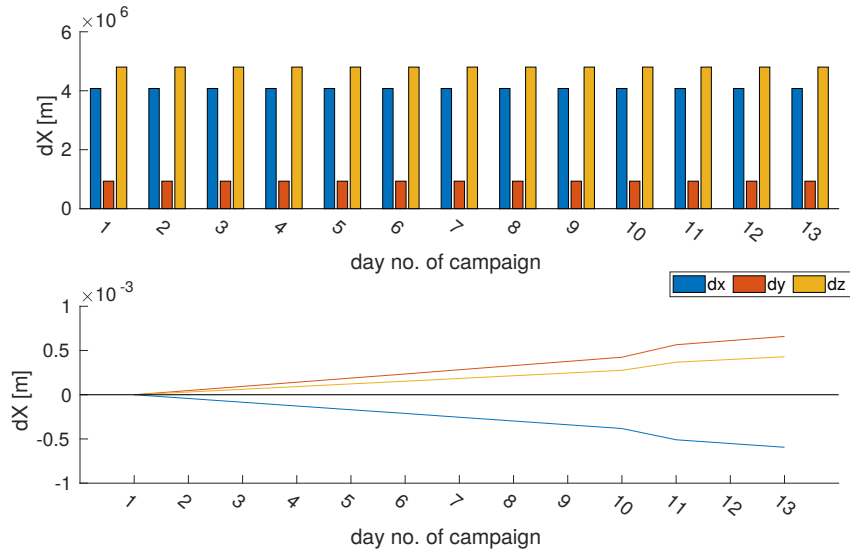
Figure 20: Daily a priori coordinates at Wettzell SLR station. The upper plot shows the absolute values. The lower plot shows the development over the course of the measuerment campaign.

ad **Processing/Results:**

During the estimation of the technique-specific solutions, daily residuals were estimated as intermediate results. Their developement over the course of the campaign at one station was presented in chapter 7.1 and 7.2. Figure 21 and 22 show the corresponding residuals for day 1 at all stations.
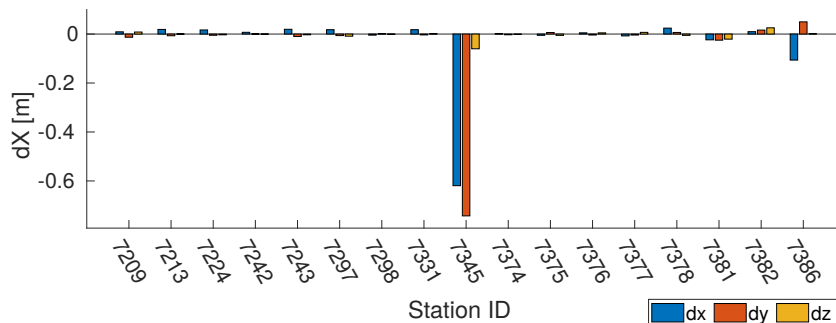
Figure 21: Residuals for VLBI stations; derived for day 1 of CONT14.
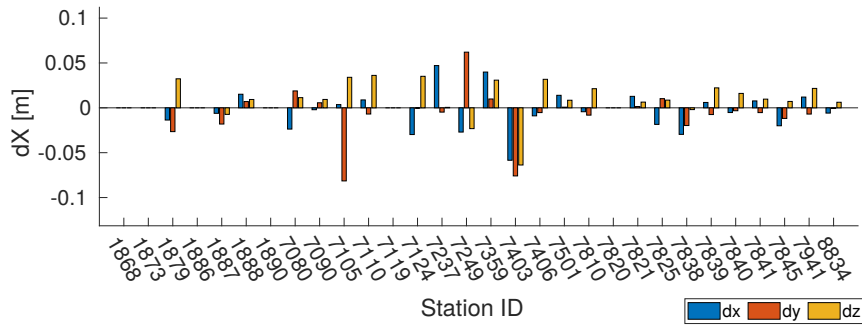
Figure 22: Residuals for SLR stations; derived for day 1 of CONT14.

ad **Results - Combination *Option 3*:**

As mentioned in chapter 7.3, defining the geodetic datum for a combined solution with a priori coordinates from the reference systems from different space geodetic techniques yields extreme distortions and questionable result. However, figure 23 and 24 show the respective residuals.
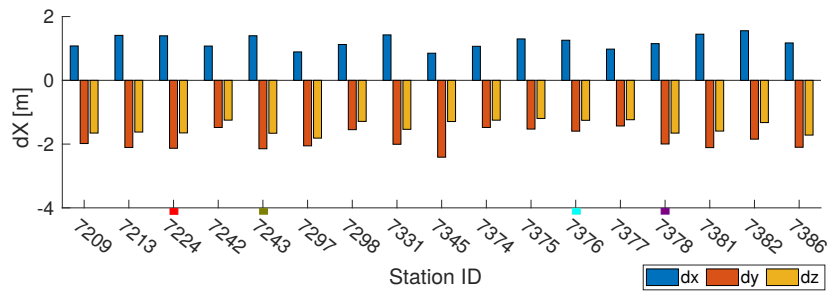
Figure 23: Residuals for VLBI stations; derived for a combined solution, including 4 local ties and defining the datum with VLBI and SLR stations.
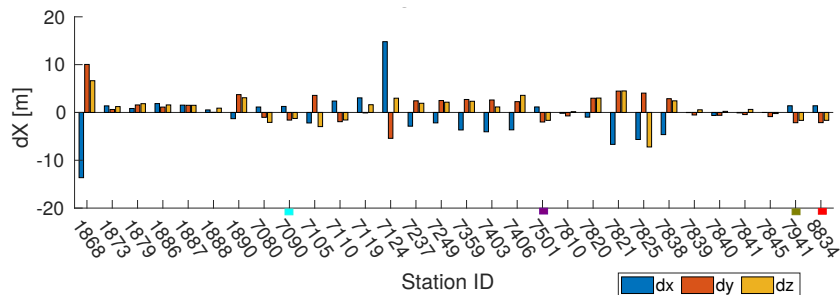
Figure 24: Residuals for SLR stations; derived for a combined solution, including 4 local ties and defining the datum with VLBI and SLR stations.

56

B. List of Figures

C. List of Tables

D. Glossary

ITRS International Terrestrial Reference System

IERS International Earth Rotation and Reference Sytems Service

ITRF International Terrestrial Reference Frame

DTRF Deutscher geodätischer terrestrischer Referenzrahmen

TRF Terrestrial Reference Frame

IGN Institut Géographique National

DGFI Deutsches Geodätisches Forschungsinstut

NEQ normal equation

VLBI Very Long Baseline Interferometry

SLR Satellite Laser Ranging

GNSS Global Navigation Satellite System

DORIS Doppler Orbitography and Radiopositioning Integrated by Satellite

EOP Earth Orientation Parameter

GPS Global Positioning System

GLONASS Globalnaya Navigatsionnaya Sputnikovaya Sistema

CNES Centre National D'études Spatiales

ESA European Space Agency

SINEX Solution INdependent EXchange Format

CONT14 Continous VLBI Campaign 2014

IVS International VLBI Service

BKG Bundesamt für Kartographie und Geodäsie

ASI Agenzia Spaziale Italiana

LSA Least Squares Adjustment

GM Gauss-Markoff Model

NNT no-net-translation

NNR no-net-rotation

IVS International VLBI Service Geodesy & Astronomy

ILRS International Laser Ranging Service

VTRF VLBI Terrestrial Reference Frame

SLRF SLR Reference Frame

GGOS Global Geodetic Observing System

GRACE Gravity Recovery and Climat Experiment

E. References

Altamimi, Z., Rebischung, P., Métivier, L., and Collilieux, X. (2016). Itrf2014: A new release of the International Terrestrial Reference Frame modeling nonlinear station motions. *Journal of Geophysical Research: Solid Earth*, 121(8):6109–6131. 2016JB013098.

Angermann, D., Drewes, H., Krügel, M., Meisel, B., Gerstl, M., Kelm, R., Müller, H., Seemüller, W., and Tesmer, V. (2004). ITRS Combination Center at the DGFI: A Terrestrial Reference Frame Realization 2003. (313):144.

Bauer, M. (2011). *Vermessung und Ortung mit Satelliten: Globale Navigationssatellitensysteme (GNSS) und andere satellitengestützte Navigationssysteme*. Wichmann Heidelberg.

Biancale Richard, Arnaud Pollet, David Coulot, M. M. (2017). E-GRASP/Eratosthenes: a mission proposal for millimetric TRF realization. 19:8752.

Böhm, J. (2014). *Moderne Geodätische Weltraumverfahren - Lecture notes, Vienna UT*.

Gérard, P. and Luzum, B. (2010). IERS Conventions (2010). *Bureau International Des Poids Et Mesures Sevres (France)*, pages 1–179.

Glaser, S., König, R., Ampatzidis, D., Nilsson, T., Heinkelmann, R., Flechtner, F., and Schuh, H. (2017). A global terrestrial reference frame from simulated VLBI and SLR data in view of GGOS. *Journal of Geodesy*, 91(7):723–733.

Hobiger, T. and Otsubo, T. (2014). Combination of GPS and VLBI on the observation level during CONT11—common parameters, ties and inter-technique biases. *Journal of Geodesy*, 88(11):1017–1028.

IVS Website (2014). Web: Continuous VLBI Campaign 2014 - https://ivscc.gsfc.nasa.gov/program/cont14/, accessed on March, 20th, 2018.

Leick, A., Rapoport, L., and Tatarnikov, D. (2015). GNSS Positioning Approaches. *GPS Satellite Surveying, Fourth Edition*, pages 257–399.

Navratil, G. (2006). *Ausgleichungsrechnung II - Lecture notes, Vienna UT*.

Niemeier, W. (2008). Ausgleichungsrechnung: Statistische auswertemethoden.

Plank, P. (2016). Comparison of analysis strategies for the determination of the ITRF. *Vienna UT*.

Pontius, R. G., Thontteh, O., and Chen, H. (2008). Components of information for multiple resolution comparison between maps that share a real variable. *Environmental and Ecological Statistics*, 15(2):111–142.

Schuh, H. and Behrend, D. (2012). VLBI: A fascinating technique for geodesy and astrometry. *Journal of Geodynamics*, 61:68 – 80.

Schuh, H. and Böhm, J. (2013). Very long baseline interferometry for geodesy and astrometry. In *Sciences of Geodesy-II*, pages 339–376. Springer.

Seeber, G. (2003). *Satellite geodesy: foundations, methods, and applications*. Walter de gruyter.

Seitz, M. (2015). Comparison of different combination strategies applied for the computation of terrestrial reference frames and geodetic parameter series. In *The 1st International Workshop on the Quality of Geodetic Observation and Monitoring Systems (QuGOMS'11)*, pages 57–64. Springer.

Takahashi, F. (2000). *Very Long Baseline Interferometer*. Wave summit course. Ohmsha.

Teunissen, P. and Montenbruck, O. (2017). *Springer handbook of global navigation satellite systems*. Springer.

Thaller, D. (2008). *Inter-technique combination based on homogeneous normal equation systems including station coordinates, Earth orientation and troposphere parameters*. PhD thesis, Technische Universität München.

Thaller, D., Krügel, M., Rothacher, M., Tesmer, V., Schmid, R., and Angermann, D. (2007). Combined Earth orientation parameters based on homogeneous and continuous VLBI and GPS data. *Journal of Geodesy*, 81(6-8):529–541.

Vervaeck, Armand (2014). Strong moderately dangerous earthquake close to Ito, Japan (greater Tokyo area).

Wolf, P. R. and Ghilani, C. D. (1997). *Adjustment computations: statistics and least squares in surveying and GIS*. Wiley-Interscience.

Xu, G. and Xu, Y. (2016). *GPS: theory, algorithms and applications*. Springer.